

The Role of Topography in the Emergence of African Savannas

by

Yeonjoo Kim

B.S., Civil and Urban Engineering, Yonsei University (2001)

Submitted to the Department of Civil and Environmental Engineering
in partial fulfillment of the requirements for the degree of

Master of Science in Civil and Environmental Engineering

at the

MASSACHUSETTS INSTITUTE OF TECHNOLOGY

September 2003

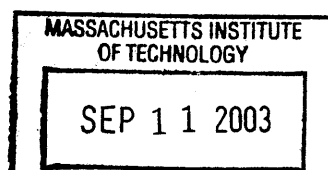
© Massachusetts Institute of Technology 2003. All rights reserved.

Author
Department of Civil and Environmental Engineering
August 6, 2003

Certified by
Elfatih A. B. Eltahir
Professor of Civil and Environmental Engineering
Thesis Supervisor

Accepted by
Heidi Nepf
Chairman, Department Committee on Graduate Students

BARKER



The Role of Topography in the Emergence of African Savannas

by

Yeonjoo Kim

Submitted to the Department of Civil and Environmental Engineering
on August 6, 2003, in partial fulfillment of the
requirements for the degree of
Master of Science in Civil and Environmental Engineering

Abstract

The coexistence of trees and grasses in savannas are not well understood even though savannas occupy a wide area of West Africa. In this study, a hypothesis is proposed to investigate the question of how trees and grasses coexist in a region. The hypothesis suggests that the variation in elevation leads to the variation in soil moisture, which in turn can explain the coexistence of trees and grasses in savannas. To test this hypothesis, experimental simulations are performed using biospheric model, IBIS, and distributed hydrologic model, SHE. We, first, estimate the amount of rainfall required for trees and grasses under a certain atmospheric condition. Here, the variation of rainfall is prescribed to force a similar variation of soil moisture. A 30% decrease in rainfall is sufficient to simulate grasses at 9°N. A 100% increase in rainfall is sufficient to simulate trees at 11°N. However, even with a five fold increase in rainfall, the model fails to simulate trees at 13°N. To study the influences of topography explicitly, a distributed hydrologic modeling is performed using SHE. The results suggest that the variation of the depth to water table induced by the varying elevation is highly correlated with the variation of soil moisture. Consequently, an asynchronous coupling of SHE and IBIS is designed to investigate the stated hypothesis. The coupling is performed by modifying IBIS to include the groundwater table as a boundary variable. The modified IBIS simulates both trees and grasses according to a different water table boundary condition in natural savannas of 11°N. The shallow water table of valleys allows the growth of trees, and the deep water table of hills allows the growth of grasses.

The simulations in this study suggest that the variability of soil moisture resulting from the topographic variation can be a determinant of savanna ecosystems. Moreover, grasslands in 13°N cannot be changed into forests only by adjusting soil moisture. It suggests that the role of soil moisture can be significant to dictate the

vegetation type only in a certain window characteristic of savanna climate.

Thesis Supervisor: Elfatih A. B. Eltahir

Title: Professor of Civil and Environmental Engineering

Acknowledgments

I would like to express my gratitude and appreciation to my advisor, Elfatih A. B. Eltahir. I am so grateful for his support and patience on me. Without his guidance this work would not be possible.

I want to thank Pat Yeh, a former member of Eltahir research group, for his taking care of me during my first year, the sabbatical year of Fatih. Even after he left MIT, he has supported me with the instruction in academic and private life! Special thanks go to Anke Hildebrandt, a member in my research group. She have been giving me help and joy over the two years.

Finally, but most importantly, I want to thank my parent for their countless support and love. They always pray for my sake to God, and just want for me to be happy.

Contents

1	Introduction	11
1.1	Background	11
1.2	Literature Review on Savanna Dynamics	15
1.2.1	Equilibrium View	16
1.2.2	Disequilibrium View	18
1.3	New Hypothesis	18
1.4	Thesis Structure	22
2	Model Description	24
2.1	Introduction	24
2.2	Biospheric Model	25
2.2.1	Land Surface Module	27
2.2.2	Vegetation Penology Module	29
2.2.3	Carbon Balance Module	29
2.2.4	Vegetation Dynamics Module	29
2.3	Distributed Hydrologic Model	30
2.3.1	Overland Flow	30

2.3.2	Channel Flow	33
2.3.3	Evapotranspiration	34
2.3.4	Unsaturated Zone Flow	35
2.3.5	Saturated Zone Flow	36
3	Simulations Using the Biospheric Model	38
3.1	Experimental Design	39
3.1.1	Rainfall Variation Method	39
3.1.2	Model Setup	41
3.2	Results	43
3.2.1	Experimental Simulation 1: 9°N	43
3.2.2	Experimental Simulation 2: 11°N	45
3.2.3	Experimental Simulation 3: 13°N	47
3.3	Discussion and Conclusion	50
4	Simulations Using Distributed Hydrologic Model	54
4.1	Details of Simulation	54
4.1.1	Study Area	55
4.1.2	Topography	55
4.1.3	Soil Profile	57
4.1.4	Initial and Boundary Condition	57
4.1.5	Atmospheric Forcings	59
4.1.6	Soil Property	59
4.2	Results and Analyses	60

4.2.1	Influences of Depth to Water Table	65
4.2.2	Influences of Surface Lateral Flow	65
4.3	Conclusion	68
5	Simulations Using IBIS and Including Groundwater Table	72
5.1	Asynchronous Coupling of IBIS and SHE	72
5.2	Modification of IBIS	74
5.3	Details of Simulation	77
5.4	Results	79
5.4.1	Experimental Simulation 1: 11°N	79
5.4.2	Experimental Simulation 2: 13°N	79
5.5	Discussion and Conclusion	84
6	Conclusions	88
	References	92

List of Figures

1-1	USGS Land Cover Classification. Savannas are bounded by 7°N and 12.5°N roughly.	12
1-2	(a) Mean Annual Accumulated Rainfall [mm]; (b) Mean Annual Air Temperature [°C]. Based on the monthly climatology of the NCEP reanalysis data (1968-1996)	14
1-3	Illustration of New Hypothesis in the Emergence of Savannas	20
2-1	State Description of IBIS. The model includes two canopy layers and soil layers divided into six sub layers. The upper canopies extend their roots more deeply than the lower canopies in soil layers. The atmospheric boundary condition is prescribed, and the lower boundary is specified by the drainage condition. (Foley <i>et al.</i> , 1996)	26
2-2	Hierarchical Framework of IBIS. In a common grid cell, each module operates on different time step. Its results are incorporated with others to the direction of arrows. (Foley <i>et al.</i> , 1996)	28
2-3	Schematic Representation of the SHE ©DHI	31

3-1	Change of the leaf area index (LAI) of the lower and upper canopy during the simulations at 9°N. The two different types of vegetation, lower canopy (grass) and upper canopy (tree), are resolved regard to the amount of total annual rainfall rates.	44
3-2	Change of the leaf area index (LAI) of the lower and upper canopy during the simulations at 11°N	46
3-3	Seasonal cycle of precipitation at 13°N from NCEP/NCAR and HAPEX-Sahel	48
3-4	Change of the leaf area index (LAI) of the lower canopy during the simulations at 13°N with the data from (a) NCEP/NCAR, and (b) HAPEX-Sahel	49
3-5	Seasonal Cycle of (a) Precipitation, (b) Air Temperature, (c) Relative Humidity, (d) Fractional Cloud Cover, and (e) Wind Speed in 9, 11, and 13°N. This is used as inputs of the model.	52
4-1	The Study Area	56
4-2	Soil Discretization	58
4-3	Topography and Simulated Soil Moisture of August	62
4-4	Curvature and Simulated Soil Moisture of August	63
4-5	(a) Monthly correlations between elevation and top 1m soil moisture, and between curvature and top 1m soil moisture, (b) Elevation and top 1m soil moisture in August, and (c) Curvature and top 1m soil moisture in August	64

4-6	Simulated Depth to Water Table and Soil Moisture of August	66
4-7	(a) Monthly correlations between water table depth and top 1m soil moisture, (b) top 1m soil moisture and water table depth in August, and (c) Curvature and water table depth in August	67
4-8	Simulated Surface Lateral Flow and Soil Moisture of August	69
4-9	(a) Monthly correlations between surface lateral and top 1m soil mois- ture, (b) top 1m soil moisture and surface lateral flow in August, and (c) Curvature and surface lateral flow in August	70
5-1	Asynchronous Coupling IBIS and SHE	75
5-2	Simulated Mean Water Table Depth of 11°N	80
5-3	Annual Cycle of (a) Rainfall Rate, and (b), (c) and (d) Groundwater Table Depth of Different Means in 11 °N	81
5-4	Annual Cycle of Groundwater Table Depth, Simulating Trees (Red) and Grasses (Black) at 11 °N	82
5-5	Change of (a) Lower Canopy LAI and (b) Upper Canopy LAI in re- sponse to the Different Groundwater Table Cycle at 11 °N	83
5-6	Change of (a) Shallowest Water table of SHE simulation, and (b) Lower Canopy LAI of IBIS with NCEP/NCAR at 13 °N	85
5-7	Change of (a) Shallowest Water table of SHE simulation, and (b) Lower Canopy LAI of IBIS with HAPEX-Sahel at 13 °N	86

List of Tables

3.1	Summary of the simulations at 9°N.	43
3.2	Summary of the simulations at 11°N.	45
3.3	Summary of the simulations at 13°N.	47
3.4	Summarized Results from the Experimental Simulations	50
4.1	Soil Parameters for Unsaturated Zone	60
6.1	Summarized Results	89

Chapter 1

Introduction

1.1 Background

Savanna ecosystems are described as a mixture of trees and grasses, constituting one of the world's major biomes and occupying about 20% of the land surface of the world. They are also defined as tropical or near-tropical ecosystems with a continuous herbaceous grass layer and a discontinuous layer of trees or shrubs (Skarpe, 1992). Savannas often occupy the areas between the equatorial forests and the mid-latitude deserts as a buffer zone, their ecology is neither that of grassland, nor that of a forest (Scholes & Walker, 1993). The complex interaction of trees and grasses shapes their ecological characteristics, and the coexistence of them still remains unresolved due to its complexity.

West African Savannas are the region of interest in this study. West Africa is defined here as the region between the Sahara desert to the north and the Atlantic coast to the south, and between 15°W and 15°E longitude. Savannas occupy the

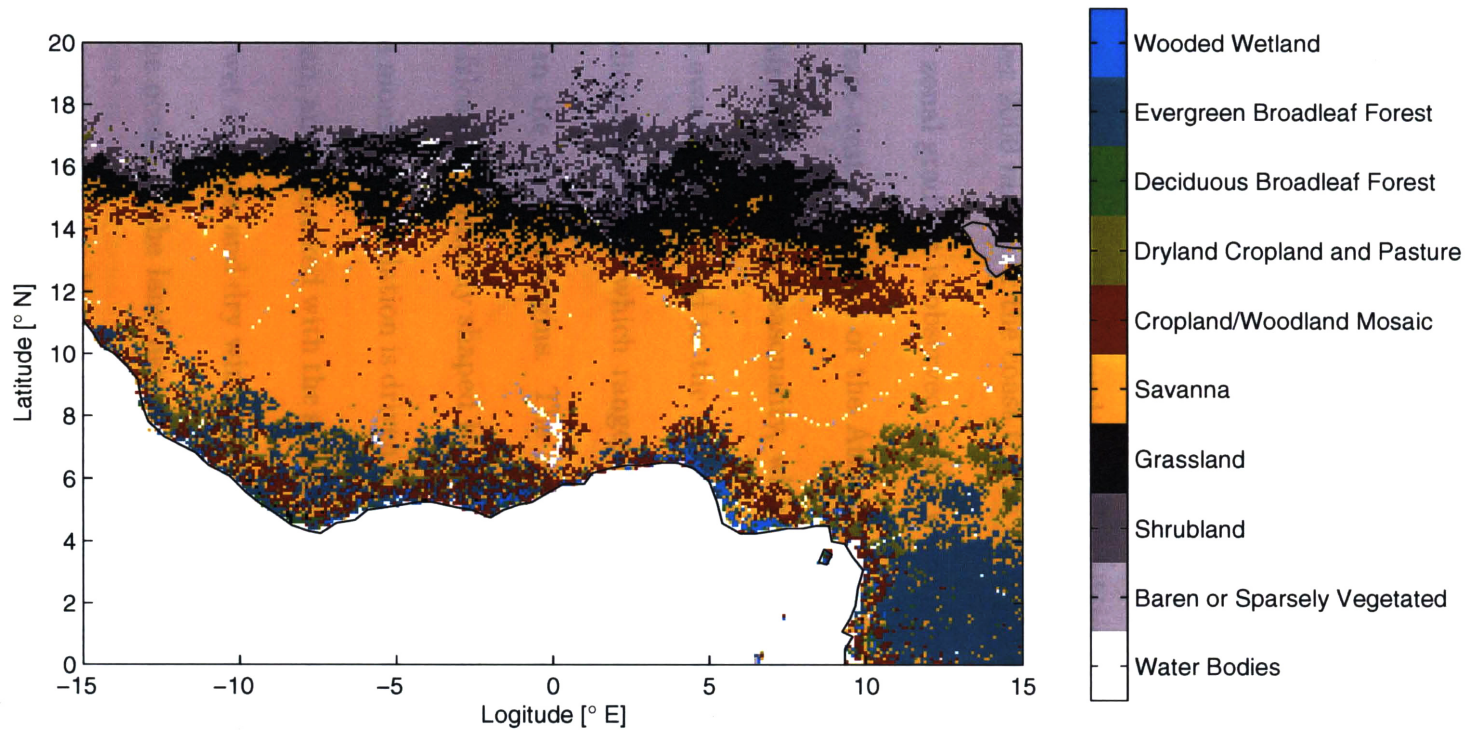


Figure 1-1: USGS Land Cover Classification. Savannas are bounded by 7°N and 12.5°N roughly.

wide areas of West Africa as seen in Figure 1-1, and are roughly bounded by 7°N and 12.5°N latitude (Anderson *et al.* , 1976; Foley *et al.* , 1996). Before focusing on West African savanna, some background on climate and land cover of West Africa is presented.

West Africa falls in the tropical climate zone, and is under the influence of the West African monsoon circulation. Rainfall is the main variable in the atmospheric dynamics of this area. The annual rainfall exhibit a sharp meridional gradient ranging from over 2000 *mm* near the coast to less than 200 *mm* on the Sahara desert border. A weak zonal gradient is observed in the western coast. The rainfall contour parallels to the east-west coast line of the Atlantic Ocean as seen in Figure 1-2. Climate of West Africa has strong seasonality, with a wet summer and a dry winter. Most of rainfall events are limited to the wet season. The duration of rainy season also has a meridional gradient, which ranges from five months in the coastal region to one month in the desert margins. The zonal symmetry and the seasonal variability in West Africa are primarily shaped by the West African monsoon circulation.

The monsoon circulation is driven by the differential heating between the land and the ocean, and is marked with the seasonal shift in the wind direction. It is responsible for the wet summer and dry winter over land. During the summer season, wind moves from the ocean to the land near the surface while transporting the moist air. Then the wet air parcels are heated further leading to moist convection. This leads to the cloud formation, and the consequent rainfall events. The reverse circulation during winter sharpens the cool and dry season. The monsoon circulation is meridional in West Africa since the southern coast line is almost parallel to the equator. In turn,

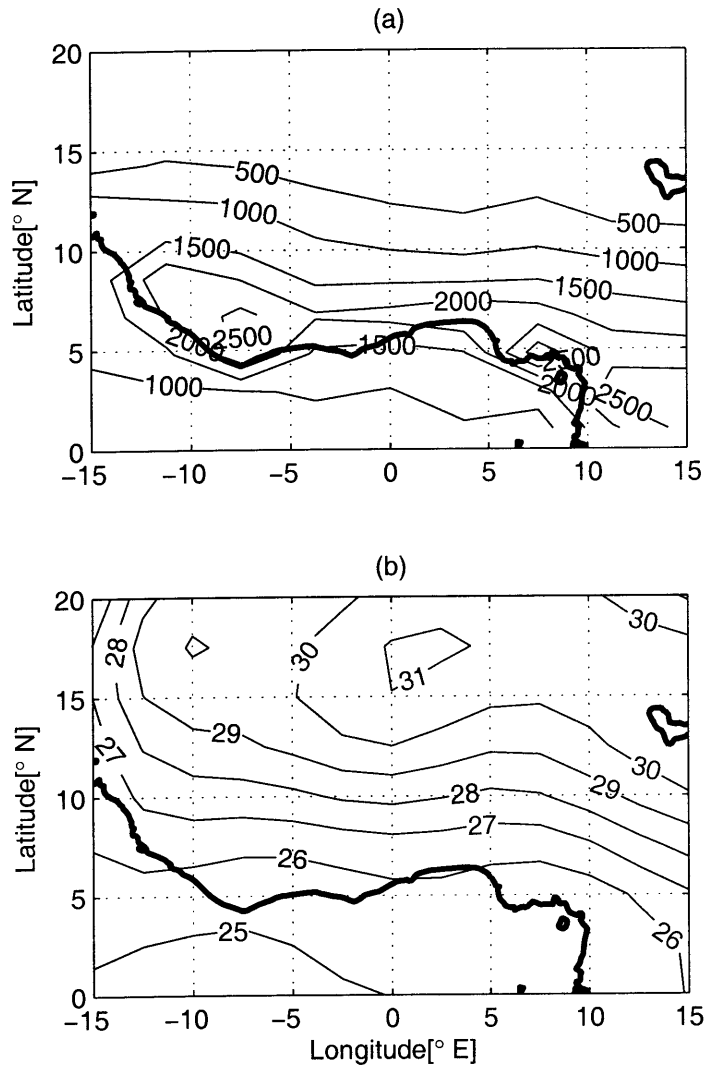


Figure 1-2: (a) Mean Annual Accumulated Rainfall [mm]; (b) Mean Annual Air Temperature [°C]. Based on the monthly climatology of the NCEP reanalysis data (1968-1996)

this is responsible for the zonal symmetry of the climate, together with the Hadley circulation.

Climate is the primary factor that dictates the distribution of vegetation. The meridional gradients of the climate variables (see Figure 1-2), make the distribution of the dominant vegetation type roughly parallel to the latitudinal line. The coastal region has access to abundant water and energy, which is enough to support trees. The amount of rainfall decreases northward, then the area around the desert border is stressed by the lack of water. Grasses can survive with relatively less water than trees since grasses transpire efficiently with shallow roots. Consequently, grasses are the dominant vegetation type in the north. In other words, the ecosystem changes from forests at the coastal region to grasslands at the northern edges. Between forests and grasslands, savannas exist as a transitional zone. As shown in Figure 1-1, savannas occupy extensive area of West Africa. But their dynamics are not as well understood as grasslands and trees. This study concentrates on how savanna exists. Then the details of savanna dynamics will be reviewed in the following section.

1.2 Literature Review on Savanna Dynamics

Savannas are characterized as grasslands with scattered trees. Herbaceous grasses and deciduous trees (or shrubs) coexist in the same region. In the classical view of the plant competition, one outcompetes the other when two different types of competitor use the same resources (e.g., energy, water, and nutrients). In savannas, however, two competitors, trees and grasses, often coexist so we are interested in what conditions

allow them survive together.

There are two theories, which are described here as the equilibrium and disequilibrium views. The first theory suggests savannas are a stable ecosystem equilibrium that is a result of competition between trees and grasses for the resources such as soil water, light and nutrients. More recently proposed, the disequilibrium view suggests that savannas are achieved through a disturbance mechanism such as fires and grazing.

1.2.1 Equilibrium View

The equilibrium school suggests that the coexistence of different vegetation types is dynamically stable. Different species compete for water, light, and nutrients, then the equilibrium is achieved in savannas, as it is elsewhere. The focus is on the water-limited arid and semi-arid savannas. Walter (1971) hypothesizes that water is a determinant of semi-arid savannas, and the grasses only exploit the shallow soil moisture. But the trees and shrubs can access the soil water of the deep soil as well as that of the shallow soil. Based on Walter's hypothesis, several models have been developed to explain the existence of savannas. Walker *et al.* (1981) developed an analytical model, and shows a stable equilibrium in the mixture of trees and grasses. Roots of grasses are restricted to shallow soil layers, so they have priority to exploit soil water from shallow soils. Trees extend their roots to shallow and deep soil layers, but they are outcompeted by grasses in the surface soil. Consequently, grasses utilize the soil water from the surface soil, and trees from the deep soil. In turn, trees and grasses

survive together in savannas.

Furthermore, Eagleson & Segarra (1985) include the competition of trees and grasses for energy as well as water, based on a two-layer model. They add an assumption that trees have priority to solar radiation since they exist in the higher layer than grasses, above ground. Thus, trees only use water from the deep soil that grasses cannot use. But trees limit the water use of grasses by shading them from the solar radiation. Each one impacts the other through this feedback mechanism. The model results in three equilibrium states, according to specified parameters, which are forests, grasslands, and savannas. They showed that savannas are only one ecosystem, stable to perturbations such as fires.

Recently, Rodriquez-Iturbe *et al.* (1999) develop a model to address the role of spatial dynamics and climate fluctuations in the coexistence of trees and grasses. The model is validated for the savanna climate of Southern Texas. They argue that the spatial water competition must be included to investigate the coexistence of trees and grasses. The model allows the horizontal competition between trees and grasses, and between trees or grasses themselves. In the model, a square grid pixel is occupied by a tree or grass. Then, species in neighboring cells of a grid can exploit the soil water from the next cells. The water stress corresponding to the canopy densities of trees and grasses, is investigated while allowing their spatial competition for soil moisture. The results show that a mixture of trees and grasses exists under a minimum water stress, i.e., the optimal condition. Moreover, it is noted that the change of canopy in savannas is sensitive to the climate fluctuation.

1.2.2 Disequilibrium View

The disequilibrium view suggests that disturbance mechanisms play a significant role in achieving the coexistence of trees and grasses. Disturbance mechanisms prevent savannas from developing into a simple ecosystem such as grassland or a forest. Fires, droughts and grazing are suggested as disturbances from outside the ecosystem (Skarpe, 1992; Scholes & Walker, 1993; Bourliere & Hadley, 1983).

For instance, Skarpe (1992) argue the following. “Most savannas, particularly African ones, are believed to owe their existence more to the impact of fire and large herbivores than to climate, and these factors seem largely to determine the boundary between savanna and forest.”

Scholes & Walker (1993) performed a field experiment at the savannas of Nylsve, in South Africa. From measurements in the broad-leafed savanna, they found that the grass roots use subsoil water as efficiently as tree roots, and tree roots dried out the topsoil as much as grass roots alone. Therefore the competition for the available water is not important to shape savannas. Instead, they argue that savannas are achieved by fires, droughts, herbivory, frost, lightning, and wind.

1.3 New Hypothesis

To investigate how trees and grasses coexist in savannas, here we propose a new theory. Our hypothesis is that the variation in elevation leads to variation in soil moisture content, which in turn can lead to the coexistence of the different types of vegetation in savannas. Microtopography shapes a range of microclimates that can accommodate

trees and grasses. Therefore trees and savannas can coexist in savannas in response to the variability of topography, as shown in Figure 1-3 illustrates our hypothesis.

The spatial variation of soil water contents is influenced by many factors: the variations of topography, soil property, water table depth, vegetation type, and atmospheric forcings. In this study, however, the topographic effects on the soil moisture distribution are emphasized. Topography primarily influences the soil moisture distribution through the variation of relative elevation, slope, and upslope draining area. Many researchers have tried to relate the topographic characteristics with soil water quantitatively. For example, the semi-distributed hydrologic runoff model (TOPMODEL) (Baven & Kirby, 1979) uses the term, $\ln(a/\tan\beta)$ (here a is the area draining through the unit length across the grid cell, and β is the slope of the grid cell) as the wetness index (also called topographic index). It suggests that an area would be wet when it has a large drainage area and a concave slope. The local topographic characteristics are used to represent the soil wetness (moisture content), since the topography distributes water over the area through the runoff mechanism. Rain falling on the watershed is distributed through the runoff processes during and after the rainfall events. The storm runoff takes place in the form of overland flow, interflow, and subsurface flow. Then, water converges into the concave area, usually including the channels, from the convex areas of the hillslope. The relatively low elevation, hollow slope, and shallow water table make valleys wetter than hills.

Now, the ecology of grasses and trees are considered. Plants compete for light above the ground, and water and at least 20 mineral nutrients under the ground (Casper & Jackson, 1997). Underground competition for water is essential in semi-

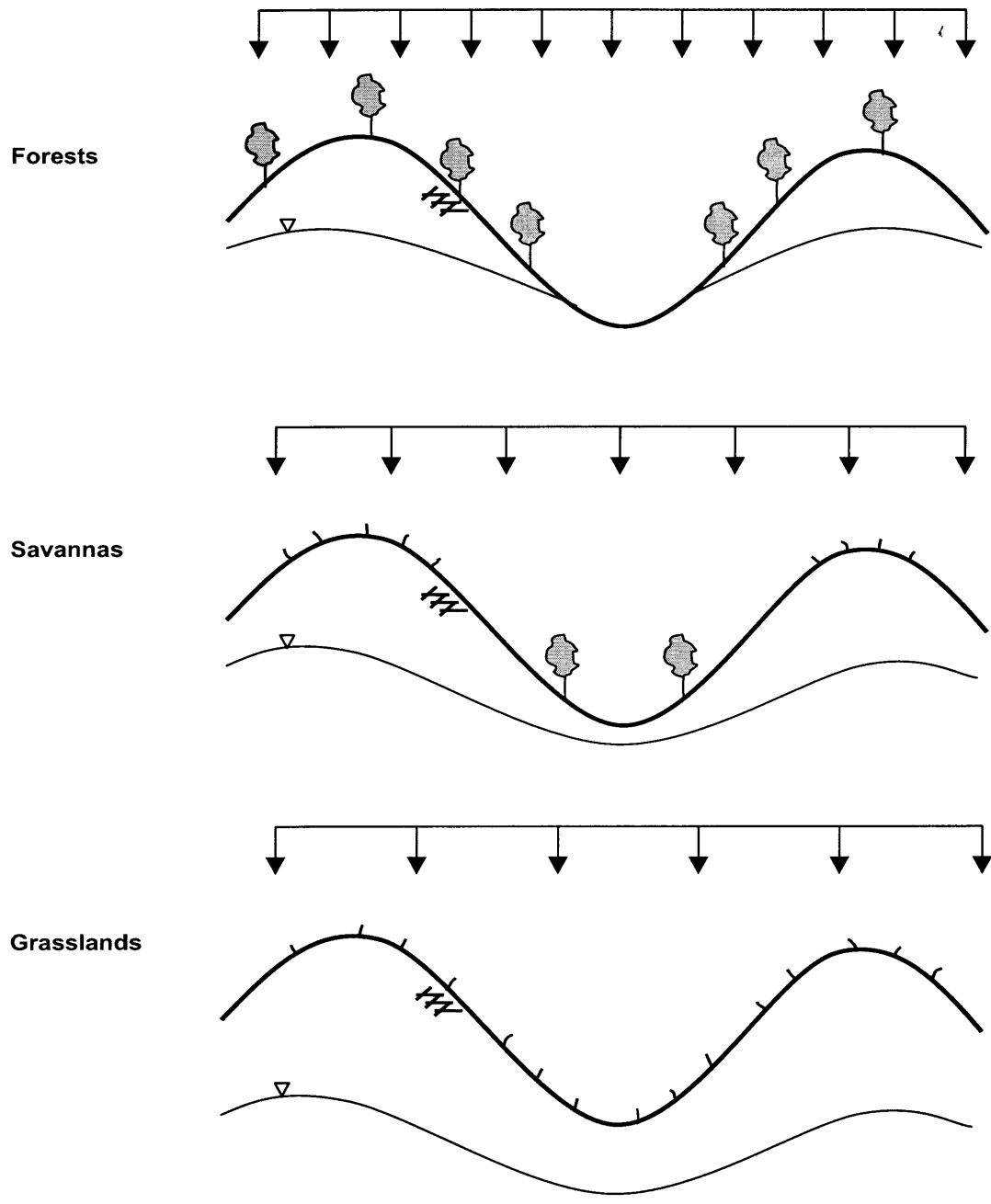


Figure 1-3: Illustration of New Hypothesis in the Emergence of Savannas

arid and arid region, where the hydrologic environment is generally unfavorable for plant existence. The water availability is particularly important there. In nature, trees and grasses compete for water, and they utilize it in different ways. Grasses transpire very actively even under water stress, i.e., they can grow under relatively low annual rainfall. Grasses just need water during the growing season. Woody plants, however, require much more water to grow, and absorb water even during the dormant period. Different climates favor different types of vegetation. For instance, the humid climate supports forests, and the dry climate supports grasslands. In savannas, however, ecologically different types of vegetation coexist under the same environments.

Finally the concave area (valleys) will have more water than convex area (hills). More moist soils in valleys can support trees, even when less moist soils in hills can be enough to support only grasses. Hence, trees and grasses can coexist in savannas in response to the variation of elevation, even under the same climate condition. To summarize, the variation of topography induces the water redistribution over the region, and then the spatial variability of soil water, in turn, can lead to the coexistence of trees and grasses.

Our new hypothesis is studied with focus on West African Savannas. In general the effects of elevation field on the soil water content are studied with physically-based, distributed hydrologic modeling system, European Hydrological System (SHE) (Abbott *et al.* , 1986a; Abbott *et al.* , 1986b). Vegetation dynamics are investigated with the biospheric model, Integrated Biosphere Simulator (IBIS) (Foley *et al.* , 1996). The two models are combined asynchronously to address our hypothesis about savanna

dynamics.

1.4 Thesis Structure

This thesis is composed of six chapters. Chapter 1 is an introduction. Savanna ecosystems and West African savannas are introduced to give the background about the research presented in this thesis. Also the previous studies on the savanna dynamics are reviewed. Finally, the new hypothesis on the emergence of savannas is proposed, which is studied throughout the thesis. Chapter 2 introduces the models used in this study. The biospheric model (IBIS) and distributed hydrologic model (SHE) are described extensively.

Chapter 3 presents the results of the simulations using the biospheric model. A section is assigned to describe the design of simulations. Then, the results of simulations are presented and discussed in the three regions, located at 9°N, 11°N and 13°N.

Chapter 4 is devoted to the distributed hydrologic modeling works. To understand the details of the hydrologic process over savannas, the physically-based distributed model (SHE) is used. To concentrate on the redistribution of soil water in the response to the variation of topography, the simulations are performed assuming hypothetical conditions, such as homogeneous soil and uniform rainfall distribution over the domain. From the simulation results, several hydrologic variables (e.g., the top soil water and depth to water table) and their correlations are presented. In conclusion, we shed a light on how topography plays a role in distributing the water under the

semi-arid savannas.

Chapter 5 describes the simulations performed with the modified IBIS. From Chapter 4, it is noted that the depth to the groundwater table is quite correlated with the soil moisture. Then, IBIS including the groundwater table as a boundary variable, is used to study the influence of groundwater table on the equilibrium vegetation. The results show that the coexistence of trees and grasses can be explained by the heterogeneity of the depth to water table. The conclusions of this study are summarized in Chapter 6.

Chapter 2

Model Description

2.1 Introduction

The new hypothesis on the existence of savannas of Chapter 1 will be studied using the biospheric model and the distributed hydrologic model. Integrated Biosphere Simulator (IBIS) (Foley *et al.* , 1996) is used as a biospheric model. IBIS integrates a wide range of biophysical, physiological, and ecological processes. The model, in particular, includes the vegetation dynamics to simulate the transient responses of vegetation cover according to environmental conditions. Here, the dynamic responses of vegetation are studied under the prescribed yearly climatology. However, the spatial hydrologic processes are not included in the current land surface transfer model (LSX) (Pollard & Thompson, 1995), used in IBIS. The model operates in a grid cell without the consideration for spatial (horizontal) variability, and the generated surface and subsurface runoff are dissipated out of the model domain. Therefore the distributed-hydrologic model will be used to compensate for the limitation due to the

lack of the spatial variability. The distributed hydrologic modeling work is performed with Systeme Hydrologique Europeen (SHE) (Abbott *et al.* , 1986a; Abbott *et al.* , 1986b). The SHE simulates all of the processes in the land phase of the hydrologic cycle: precipitation, evapotranspiration, including canopy interception, overland sheet flow, channel flow, unsaturated sub-surface flow, and saturated groundwater flow. These water movements are modeled based on the physical equations or empirical equations over the basin, to describe the details of all hydrologic processes. The SHE modeling framework gives us understanding of how topography plays a role to distribute the water under the environment of savannas. The following two sections are devoted to describe the details of the IBIS and the SHE.

2.2 Biospheric Model

The IBIS models an extended range of terrestrial processes under the given atmospheric conditions. The latter include air temperature, precipitation, specific humidity, relative humidity and fraction of cloud cover. The solar and longwave radiation is calculated for the specific latitude and longitude. The atmospheric forcings can be prescribed or updated through the feedback between IBIS and an atmospheric model. An atmospheric model such as any General Circulation Model (GCM) can be coupled with IBIS, which means that the results of the atmospheric model serve as the inputs to IBIS, and vice versa, continuously during the simulation.

The vegetation cover of IBIS is described by a combination of plant functional types (PFTs). The plant functional types are defined, based on ecological char-

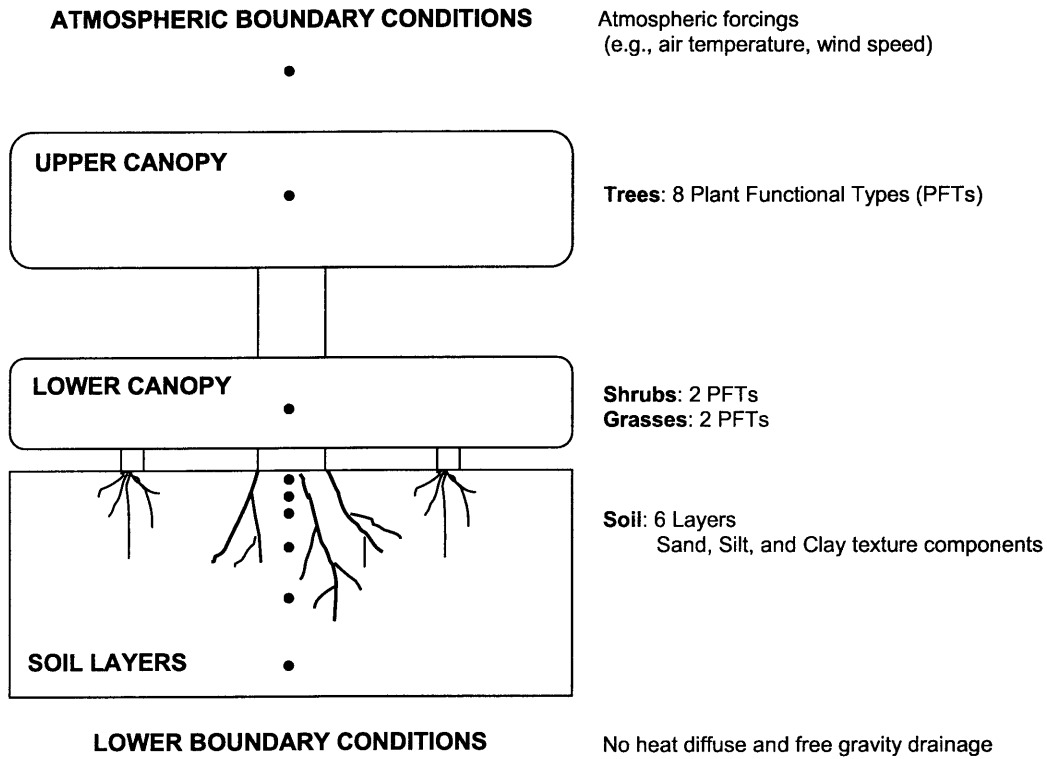


Figure 2-1: State Description of IBIS. The model includes two canopy layers and soil layers divided into six sub layers. The upper canopies extend their roots more deeply than the lower canopies in soil layers. The atmospheric boundary condition is prescribed, and the lower boundary is specified by the drainage condition. (Foley *et al.* , 1996)

acteristics: physiognomy (trees and grasses), leaf habit (evergreen and deciduous), photosynthetic pathway (C_3 and C_4), and leaf form (broad-leaf and needle-leaf). The vegetation canopy is divided into two layers, with the woody plant functional types in the upper canopy and herbaceous plant functional types in the lower canopy. The vegetation canopies extend their roots into the soil layers with canopy-specific root density distribution. The soil layers are divided into six layers with top-to-bottom thickness of 0.1, 0.15, 0.25, 0.5, 1.00, and 2.00 m. Their texture is represented by the percentage of sand, silt and clay. Figure 2-1 describes the state of IBIS.

IBIS has hierarchical and modular structure with four modules: the land surface module, vegetation phenology module, carbon balance, and vegetation dynamics module. These are independent, operate on different timesteps, and then linked, as presented in Figure 2-2.

2.2.1 Land Surface Module

This model simulates the biophysical and physiological process on a time step between 10 and 60 min (60 minutes in this study), based on the LSX land surface model (Pollard & Thompson, 1995). It exchanges energy, water vapor, carbon dioxide, and momentum between surface, the vegetation canopies, and the atmosphere. The wind regime is modeled with mixing length logarithmic profiles above and between layers, and a simple diffusion model of air motion within each layer. Total evapotranspirations include evaporation from the soil surface, evaporation of water intercepted by vegetation canopies, and canopy transpiration. Soil model simulates heat and mois-

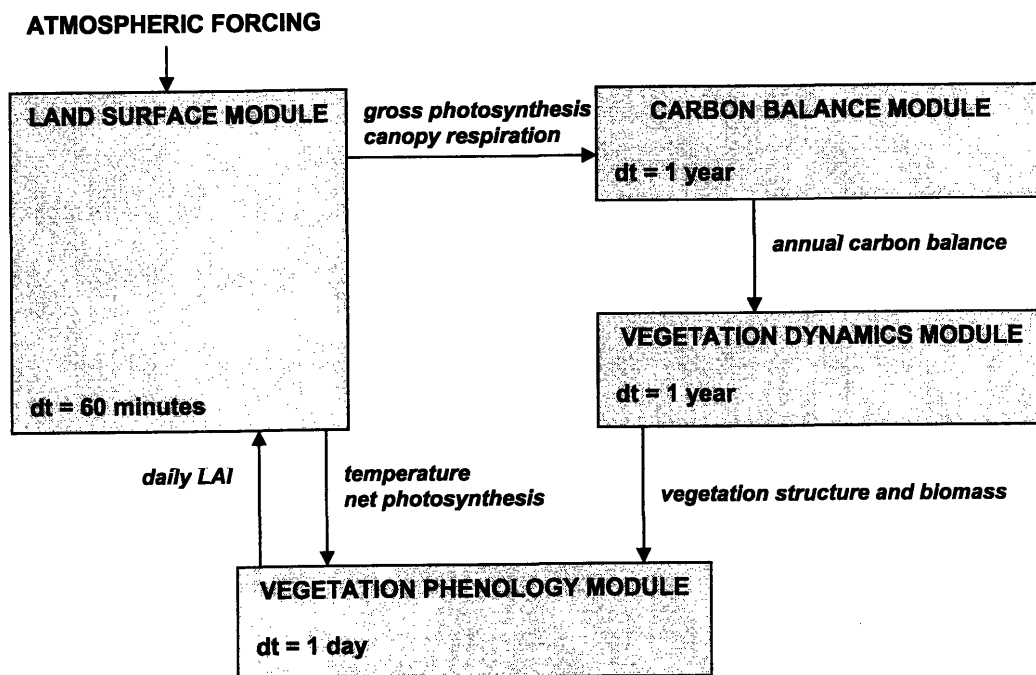


Figure 2-2: Hierarchical Framework of IBIS. In a common grid cell, each module operates on different time step. Its results are incorporated with others to the direction of arrows. (Foley *et al.* , 1996)

ture movement in upper few meters of soil. Six soil layers are represented by three variables: temperature, soil moisture and soil ice. Soil water movement is calculated by Richard's equation. For the soil bottom boundary, the gravity drainage condition is controlled by an empirical coefficient, multiplying the unsaturated hydraulic conductivity.

2.2.2 Vegetation Penology Module

The vegetation penology module describes the behavior of specific plant types in relation to seasonal climate conditions on a daily time step. The winter-deciduous and drought-deciduous behaviors of particular vegetations are modeled, and deciduous vegetations drop their leaf based on the temperature threshold or carbon balance.

2.2.3 Carbon Balance Module

This module sums photosynthesis, and growth and maintenance respiration to calculate the annual carbon balance for each PFTs. It also calculates net primary productivity (NPP) of each PFTs, which is allocated into leaves, transport tissues, and fine roots.

2.2.4 Vegetation Dynamics Module

The vegetation dynamics module simulates changes in vegetation cover on an annual time step. Each PFTs are characterized by their ability to capture resources, light and water. The upper canopy has priority for light, and shades the lower canopy.

However, the lower canopy can uptake soil moisture first. These are the competition mechanisms between upper canopy (trees) and lower canopy (grasses). The competition between PFTs within the same vegetation layer are simulated by the differences in ecological strategies: phenology (evergreen and deciduous), leaf form (broad-leaf and needle-leaf) and photosynthetic pathway (C_3 and C_4).

More details about IBIS are presented by Foley *et al* (1996).

2.3 Distributed Hydrologic Model

The SHE mathematically models the hydrologic processes of water movements. The spatial distribution of basin parameters, meteorological inputs and hydrologic responses are represented in a grid cell of horizontal and vertical layers (see Figure 2-3). The water movements are solved in a finite difference representation of the physical equations (the partial differential equations of mass, momentum and energy conservation) or empirical equations. The SHE calculates them using a modular structure. Each module runs independently, then links in order to exchange water among modules. (Abbott *et al.*, 1986b) Here the main modules are presented with their physical or empirical equations.

2.3.1 Overland Flow

When the net rainfall exceeds the infiltration capacity of the soil, water is ponded on the ground surface. This water is available as surface runoff, as determined by the topography and flow resistances. The water is lost due to evaporation and

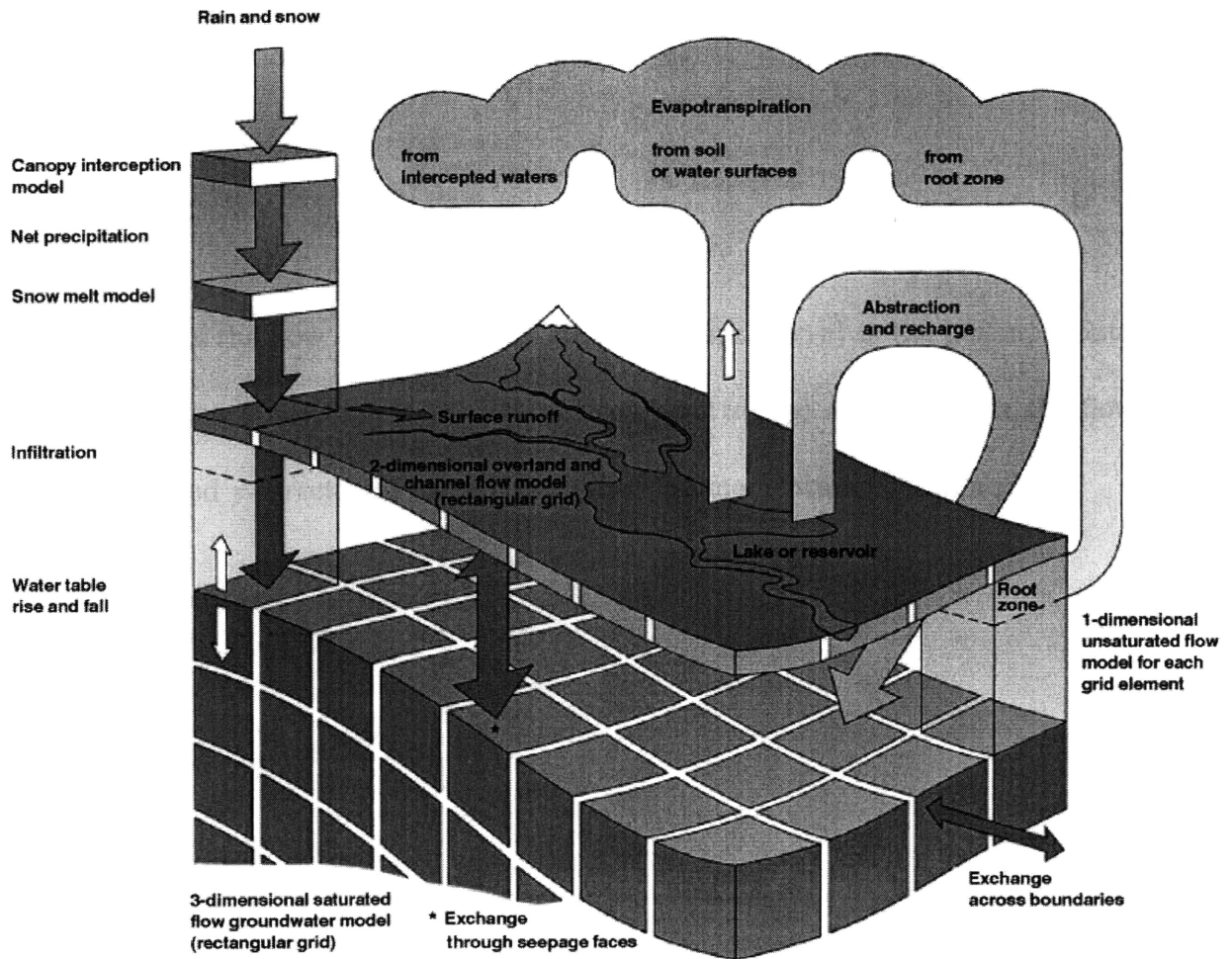


Figure 2-3: Schematic Representation of the SHE ©DHI

infiltration along the flow path, then routed into the channel.

The SHE calculates the overland sheet flow component, using the 2-D diffusive wave approximation of the Saint Venant equations. In rectangular Cartesian coordinates, the conservation of mass gives

$$\frac{\partial h}{\partial t} + \frac{\partial}{\partial x} (uh) + \frac{\partial}{\partial y} (vh) = i \quad (2.1)$$

where $h(x, y)$ is the flow depth over the ground surface, $i(x, y)$ is the net input into the overland flow (net rainfall less infiltration), and $u(x, y)$ and $v(x, y)$ is the flow velocity in x- and y-directions, respectively. And the momentum equation gives

$$S_{fx} = S_{Ox} - \frac{\partial h}{\partial x} - \frac{u}{g} \frac{\partial u}{\partial x} - \frac{1}{g} \frac{\partial u}{\partial t} - \frac{q}{g} \frac{\partial u}{\partial h} \quad (2.2a)$$

$$S_{fy} = S_{Oy} - \frac{\partial h}{\partial y} - \frac{v}{g} \frac{\partial v}{\partial y} - \frac{1}{g} \frac{\partial v}{\partial t} - \frac{q}{g} \frac{\partial v}{\partial h} \quad (2.2b)$$

where S_f is the friction slopes in the x- and y-directions, and S_O is the slope of the ground surface.

The solution of the two dimensional St. Venant equations is numerically challenging. Therefore, the momentum losses and lateral inflows perpendicular to the flow direction are ignored. Furthermore, it is assumed that the friction slope is equal to the slope of the ground surface. This is known as the kinematic wave approximation.

For each friction slope, a Strickler/Manning law is adapted with Strickler coeffi-

coefficients K_x and K_y in the two directions,

$$S_{fx} = \frac{u^2}{K_x^2 h^{4/3}} \quad (2.3a)$$

$$S_{fy} = \frac{v^2}{K_y^2 h^{4/3}} \quad (2.3b)$$

Therefore, the relation between the velocities and the depths are written as

$$uh = K_x \left(-\frac{\partial z}{\partial x} \right)^{1/2} h^{5/3} \quad (2.4a)$$

$$vh = K_y \left(-\frac{\partial z}{\partial x} \right)^{1/2} h^{5/3} \quad (2.4b)$$

where x is the ground surface. It is noted that uh and vh represent discharge per unit area.

2.3.2 Channel Flow

For the channel flow, the various components of the SHE are coupled to DHI's river hydraulic program MIKE 11. MIKE 11 do the one-dimensional simulation of river flows water levels using the fully dynamic Saint Venant equations (for details, refer to MIKE11 User Guide). The surface water and aquifer of MIKE SHE are exchanged with MIKE 11. If the area-inundation option is used, SHE calculates the distribution of surface water by comparing MIKE 11 water level with topographic elevations. The river-aquifer exchange is calculated in the grid cells adjacent to river links. The amount of exchange flux is calculated based on a conductance and a head difference

using Darcy's Law. The river-aquifer exchange is calculated when the river width is smaller than the grid size in the SHE. The flux, Q , between saturated zone grid cell and the river link is a conductance, C , multiplied by the head difference between the river and the grid cell.

$$Q = \Delta h \cdot C_{river-aquifer} \quad (2.5)$$

The conductance depends on the conductivity of the aquifer material only, that of the river bed material only, or that of the river bed and the aquifer materials.

2.3.3 Evapotranspiration

This component uses meteorological (potential evapotranspiration) and vegetative data (leaf area index and root distribution function). The processes are separately modeled with interception of rainfall by the canopy, drainage from the canopy to the soil surface, evaporation from the canopy surface, evaporation from the soil surface, and uptake of water by plant roots and its transpiration. In this study, we assume the surface as the bare soil, then only the soil evaporation is presented here. In the absence of vegetation, the soil evaporation model of Kirstensen and Jensen is simplified into the following:

$$E_s = E_p \cdot (f_3(\theta) + f_4(\theta) - f_3(\theta)f_4(\theta)) \quad (2.6a)$$

$$f_3(\theta) = \begin{cases} C_2 & \text{for } \theta \geq \theta_W \\ C_2 \frac{\theta}{\theta_W} & \text{for } \theta_r \leq \theta \leq \theta_W \\ 0 & \text{for } \theta \leq \theta_r \end{cases} \quad (2.6b)$$

$$f_4(\theta) = \begin{cases} \frac{\theta - \frac{\theta_W + \theta_{FC}}{2}}{\theta_{FC} - \frac{\theta_W + \theta_{FC}}{2}} & \text{for } \theta \geq \frac{\theta_W + \theta_F}{2} \\ 0 & \text{for } \theta \leq \frac{\theta_W + \theta_F}{2} \end{cases} \quad (2.6c)$$

where E_s is the soil evaporation and E_p is the potential evapotranspiration. Also, θ is the volumetric soil moisture content, θ_{FC} is that at field capacity, θ_W is that at the wilting point, and θ_r is the residual soil moisture content. The SHE restricts soil evaporation to the upper node in the unsaturated zone, generally about 10 *cm* deep or less.

2.3.4 Unsaturated Zone Flow

The unsaturated zone model interacts with both the overland flow and the ground water model, and acts as the link between them. Unsaturated flow is usually heterogeneous and characterized by cyclic fluctuations in the soil moisture as water is replenished and removed. Unsaturated flow is primarily vertical since gravity plays the major role during infiltration. The solutions of vertical flow are provided by the full Richards equation, a simplified gravity flow equation, or a simple two-layer water balance method. Here the most accurate equation, the full Richards equation, is used

in the tension-based form as the following:

$$C \frac{\partial \psi}{\partial t} = \frac{\partial}{\partial z} \left(K \frac{\partial \psi}{\partial z} \right) + \frac{\partial K}{\partial z} - S \quad (2.7)$$

where z is a elevation head (positive upwards), ψ is the pressure head (which is negative with the capillary force), K is the hydraulic conductivity, C is the slope on soil moisture tension curve, and the sink term S are calculated from the root extraction for the transpiration in the upper part of the unsaturated zone.

2.3.5 Saturated Zone Flow

The saturated zone component calculates the saturated subsurface flow. The SHE allows for a fully three dimensional flow in a heterogeneous aquifer with shifting conditions between unconfined and confined conditions. The spatial and temporal variation of the hydraulic head is described by the non-linear Boussinesq equation. The boundary flow from the other components is regarded as sources/sinks in the equation:

$$\frac{\partial}{\partial x} \left(K_{xx} \frac{\partial h}{\partial x} \right) + \frac{\partial}{\partial y} \left(K_{yy} \frac{\partial h}{\partial y} \right) + \frac{\partial}{\partial z} \left(K_{zz} \frac{\partial h}{\partial z} \right) - Q = S \frac{\partial h}{\partial t} \quad (2.8)$$

where K_{xx}, K_{yy}, K_{zz} are the hydraulic conductivity along the x, y and z axes, h is the piezometric head, Q is the volumetric flux per unit volume representing source/sink, and S is the specific storage coefficient.

Furthermore, MIKE SHE User Guide and MIKE 11 User Guide provide the de-

tailed description of the governing equation and numerical solution.

Chapter 3

Simulations Using the Biospheric

Model

This chapter presents the preliminary work to test the hypothesis of Chapter 1. The theory that the variation of elevation redistributes the water over a region and the resulting heterogeneity of soil water can explain the coexistence of trees and grasses, will be examined using a dynamic biospheric model, IBIS, including the spatial variation of elevation implicitly, without using the distributed hydrologic model at this stage.

3.1 Experimental Design

3.1.1 Rainfall Variation Method

Our theory predicts that any model should simulate a mixed vegetation type in response to the variation of water availability that is triggered by the elevation variability, over naturally-found savannas. To use the IBIS for this study, however, the model has two limitations.

First, IBIS does not simulate a savanna as an equilibrium land cover over West Africa. The model evolves into the equilibrium with tropical deciduous forests in 9°N, and grasslands in 11°N, but savannas are observed in 9°N and 11°N in nature (see Figure 1-1).

The disagreement of model results has been attributed to the lack of disturbance mechanism, such as fire, and interannual climate variability (Foley *et al.*, 1996). To validate the argument, Wang (2000) performed the simulations with a certain degree of fire and grazing effect on the savanna and grassland region using IBIS. It is assumed that fires take place every year during the dry season and consume a 0% to 10% of the above-ground biomass, which is randomly generated with the uniform distribution. Grazing consumes 50% of grasses every year. Under these assumptions, the model simulates a savanna-type vegetation. This result supports the disequilibrium view about the savanna dynamics. Therefore without the disturbance and interannual fluctuation of the atmospheric forcing (we use climatology as atmospheric conditions), IBIS gives a simple equilibrium state, grasslands or forests, over the West African savannas.

Second, the model assumes a flat plain over the domain. Thus we need to implement the concept of distributed hydrologic modeling into IBIS. To describe the spatial variability, one grid cell must be split into smaller pieces. Then the water exchange among neighboring cells has to be considered. In reality, this model is not developed due to its complexity and time constraints. Instead of presenting the variation of elevation directly, we vary the amount of rainfall as the input. The variation of rainfall inputs is a surrogate for the difference of soil water contents at different areas, over the region having the elevation variation. A hill area will have less soil water than a valley area since water converges to hollow valleys through runoff. Therefore more available water at a valley is represented by more rainfall input to the valley than for a hill area.

Since IBIS does not include the spatial water movement and does not resolve the savanna ecosystem as an equilibrium state, the experiments are designed to simulate the different vegetation types, grasslands or forests, while varying the amount of rainfall input. In other words, if the opposite equilibrium states (grasslands or forests) are simulated only by adjusting rainfall input amount, trees and grasses may coexist in the same region. For instance, forests are predicted in 9°N under the normal condition, then we reduce the amount of rainfall input until grasslands are simulated as an equilibrium. Furthermore, we determine the range of rainfall input amounts between valleys (where trees are resolved) and hills (where grasses are resolved). Its extent should fall into the certain range, where the variation of local topography may naturally redistribute water over the region. In addition, hereafter, the term, rainfall factor (RF) is used as the factor (e.g., 0.8, 1.2, and 1.5), multiplying the normal

amount of rainfall, which represents the effective rainfall amount reaching the area.

3.1.2 Model Setup

Our experiments are performed in three areas, 9°N , 11°N and 13°N . In natural savannas, 9 and 11°N , we expect the transition from grasslands to forests (or, from forests to grasslands) while we adjust the rainfall. Also the natural grassland area, 13°N is selected for the experiment, expecting that in this case any reasonable modification of rainfall input should not result in the transition to forests. But we do not include the forest area, the southern limit of savannas, since the rainforest area in West Africa is quite stable.

The daily climatology of air temperature, relative humidity, wind speed, precipitation and fractional cloud cover in three latitude are used for the simulations. The data are taken from the National Centers for Environmental Prediction/National Center for Atmospheric Research (NCEP/NCAR) Reanalysis Project. The data during 1958-1997 is averaged between 15°W and 15°E , then the longitude is specified with 0°E in the model. Supplemental rainfall data is taken from HAPEX-Sahel project (1991-1994) for the area of 13°N . The simulations in 13°N are done twice with NCEP/NCAR reanalysis data and with HAPE-Sahel field data. The daily temperature and specific humidity is interpolated to an hourly resolution assuming a sinusoidal diurnal cycle. The daily precipitation is assumed to occur within a certain period, which is determined by random sampling from the statistical distribution.

As pointed out before, IBIS can be coupled with the atmospheric model. By

the coupling, the model receives the feedback from the atmospheric process in response to the terrestrial biospheric model, and vice versa. In this study, however, the IBIS is used without the interaction between atmospheric and biospheric model. Although the lack of feedback between them is unrealistic, it is deemed reasonable here since our objectives are to study what hydrologic conditions help determine the savanna ecosystem, not how the atmospheric and biospheric processes are interacting in savannas.

In the beginning of simulations, all types of PFTs have the same minimal LAIs of 0.1, called “cold start” in IBIS. Each type of vegetation has equal opportunity to survive at the start time, and then they compete with others for the water and lights under the given atmospheric condition. When IBIS is coupled with the atmospheric model, the selection of initial vegetation type influences the equilibrium state (Kiang & Eltahir, 1999; Wang & Eltahir, 2000a; Wang & Eltahir, 2000b). But the initial distribution of vegetation does not influence the reached equilibrium ecosystem in our experiment, since we prescribe the daily climatology without the interaction from the atmospheric model.

Simulations run for 250 to 500 years to give enough time to reach the equilibrium state. We determine if the model is close to the equilibrium by monitoring the annual change of LAI of upper and lower canopies. A stable evolution of LAIs means that the model reached the equilibrium state.

3.2 Results

3.2.1 Experimental Simulation 1: 9°N

The model predicts the dry deciduous forests under the normal rainfall events at 9°N. Therefore we are now investigating the soil water level in valleys. To determine the rainfall rate where the transition to grasses takes place, the total annual rainfall is decreased gradually. With 0.7 times the typical rainfall amounts, the transition from forests to grasslands takes place and Table 3.1 summarizes the results of five simulations with decreasing amount of rainfall input from the normal value.

Figure 3-1 shows the change of lower LAI and upper LAI, respectively, during the simulation. Since the model is initialized with the equal, minimal amount of seeds of all PFTs, the lower canopy vegetations flourish in the beginning of simulation. Then the canopies are adapted to the given environment, and outcompete the others. In case of RF 0.7, LAI of lower canopy stays at the constant level around 8, and LAI of upper canopy does not increase and keeps its low level. This shows grasslands are resolved as an equilibrium ecosystem with RF of 0.7.

Rainfall Factor	Annual Rainfall	Vegetation Type
1.0	1.54m	Forest
0.8	1.23m	Forest
0.7	1.08m	Grassland
0.6	0.93m	Grassland
0.5	0.77m	Grassland

Table 3.1: Summary of the simulations at 9°N.

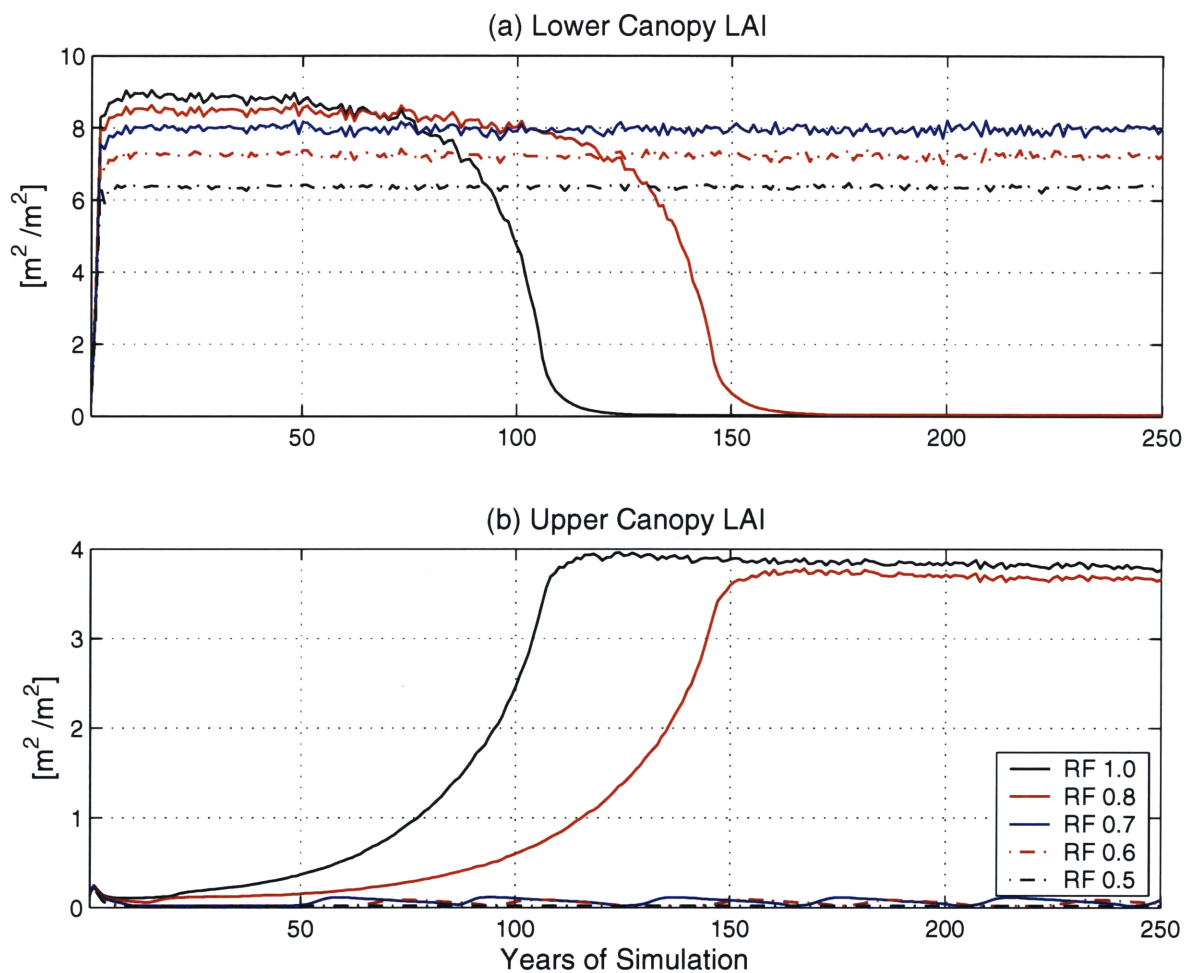


Figure 3-1: Change of the leaf area index (LAI) of the lower and upper canopy during the simulations at 9°N. The two different types of vegetation, lower canopy (grass) and upper canopy (tree), are resolved regard to the amount of total annual rainfall rates.

3.2.2 Experimental Simulation 2: 11°N

With a typical rainfall, the model resolves grassland equilibrium at 11°N. Contrary to the case of 9 °N, the annual rainfall is increased to get the transition from grasslands to forests. At RF 1.9, grasslands are resolved, and at RF 2.0 a forest equilibrium is simulated. With the annual rainfall of about 2240 *mm*, a tropical deciduous forest is simulated as an equilibrium (see Table 3.2).

As seen in Figure 3-2, LAI of lower canopy stays around 6 under the typical condition. At RF of 2.0, however, the lower canopy LAI decreases and the upper canopy LAI starts to increase after around 200 years. To confirm that the model converges to a forest equilibrium, the simulation is run for 500 years, which different from the other regions (250 years). In summary, both forests and grasslands are predicted at 11°N where savannas are naturally found, in response to the adjustment of rainfall inputs.

Rainfall Factor	Annual Rainfall	Vegetation Type
1.0	1.12m	Grassland
1.3	1.46m	Grassland
1.5	1.68m	Grassland
1.7	1.91m	Grassland
2.0	2.24m	Forest

Table 3.2: Summary of the simulations at 11°N.

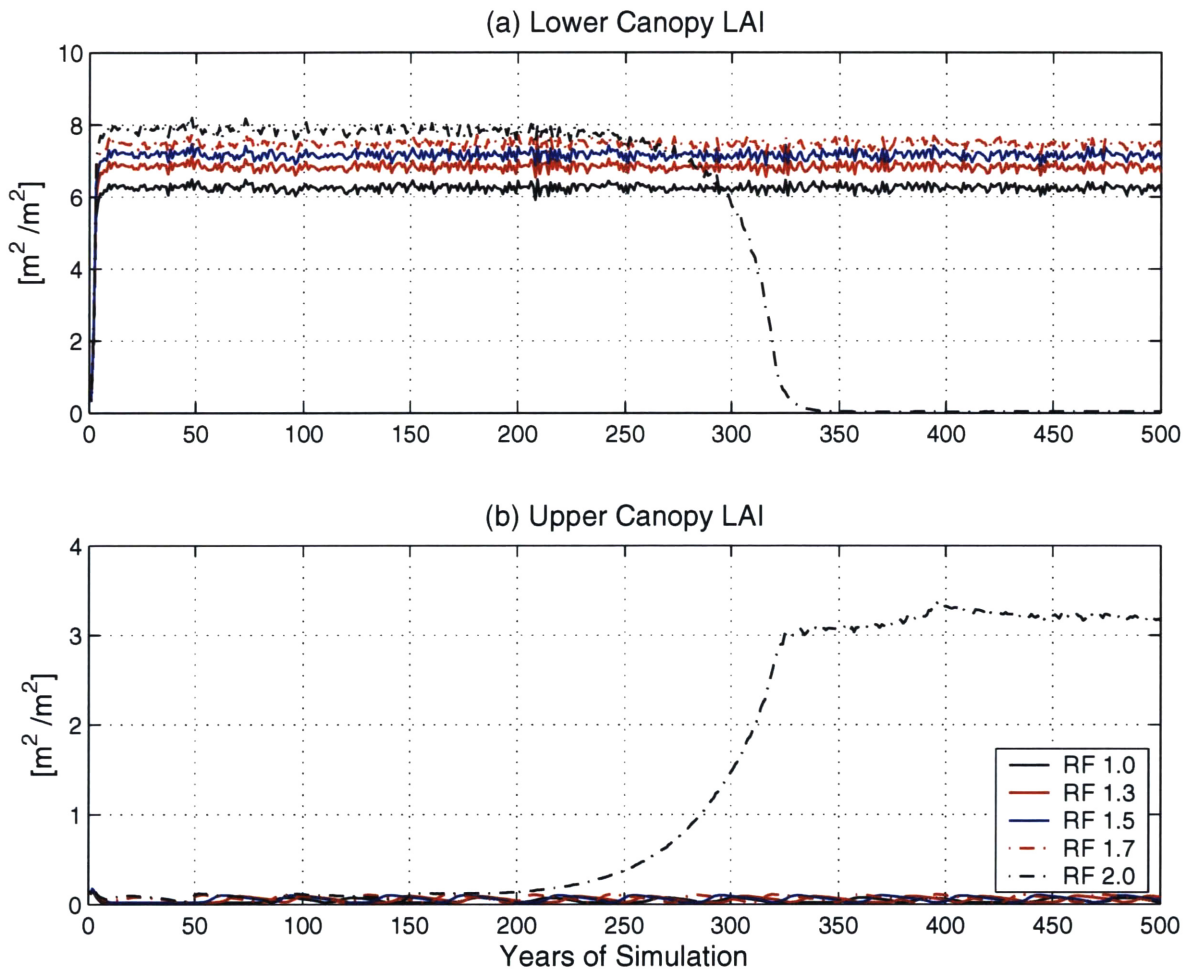


Figure 3-2: Change of the leaf area index (LAI) of the lower and upper canopy during the simulations at 11°N

3.2.3 Experimental Simulation 3: 13°N

For the case of 13°N, two sets of simulations are done. First, all the meteorological data are taken from NCEP/NCAR reanalysis project like the above cases of 9 and 11°N. Second, only the rainfall input is replaced by the measurements of HAPEX-Sahel. As seen in Figure 3-3, the measurements of rainfall show the seasonality of rainfall distribution more clearly than the reanalysis data. The annual accumulated precipitation is not much different between them, with 0.77 m and 0.69 m in NCEP/NCAR and HAPEX-Sahel, respectively. However, the data from HAPEX-Sahel shows the intense rainfall during a wet summer. The reanalysis data presents a less intense and more frequent storms through the year.

In the observations, the region in 13°N is at the north boundary of savannas and consists of grasslands. With the NCEP/NCAR climatology, the equilibrium vegetation is grassland under the normal condition. Thus the amount of rainfall input is increased to see the equilibrium under valley conditions, like 11°N. As seen in Table 3.3, the transition from grasslands to forests does not take place. We get the

	NCEP/NCAR		HAPEX-Sahel	
Rainfall Factor	Annual Rainfall	Vegetation Type	Annual Rainfall	Vegetation Type
1.0	0.77m	Grassland	0.69m	Grassland
2.0	1.54m	Grassland	1.38m	Grassland
3.0	2.31m	Grassland	2.07m	Grassland
4.0	3.08m	Grassland	2.76m	Grassland
5.0	3.86m	Grassland	3.45m	Grassland

Table 3.3: Summary of the simulations at 13°N.

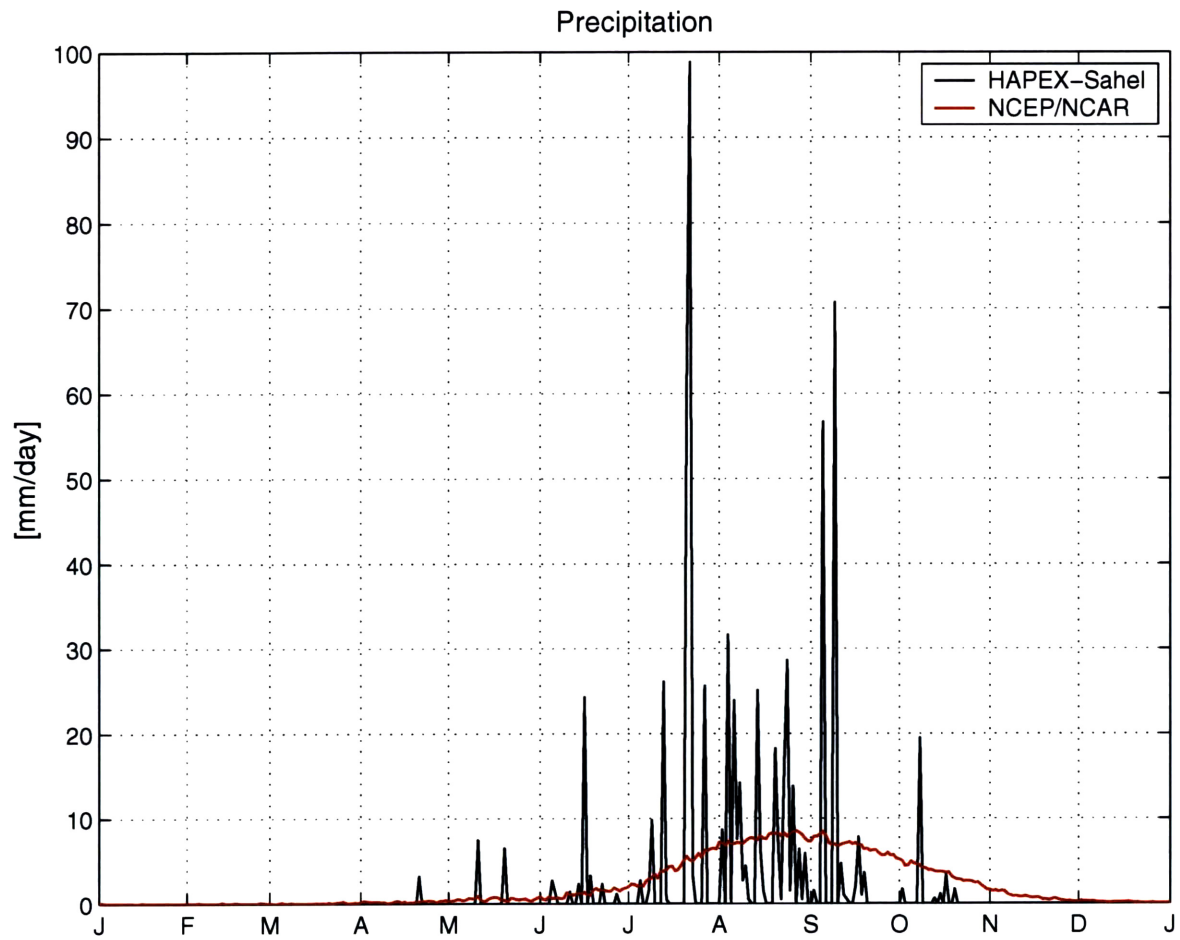


Figure 3-3: Seasonal cycle of precipitation at 13°N from NCEP/NCAR and HAPEX-Sahel

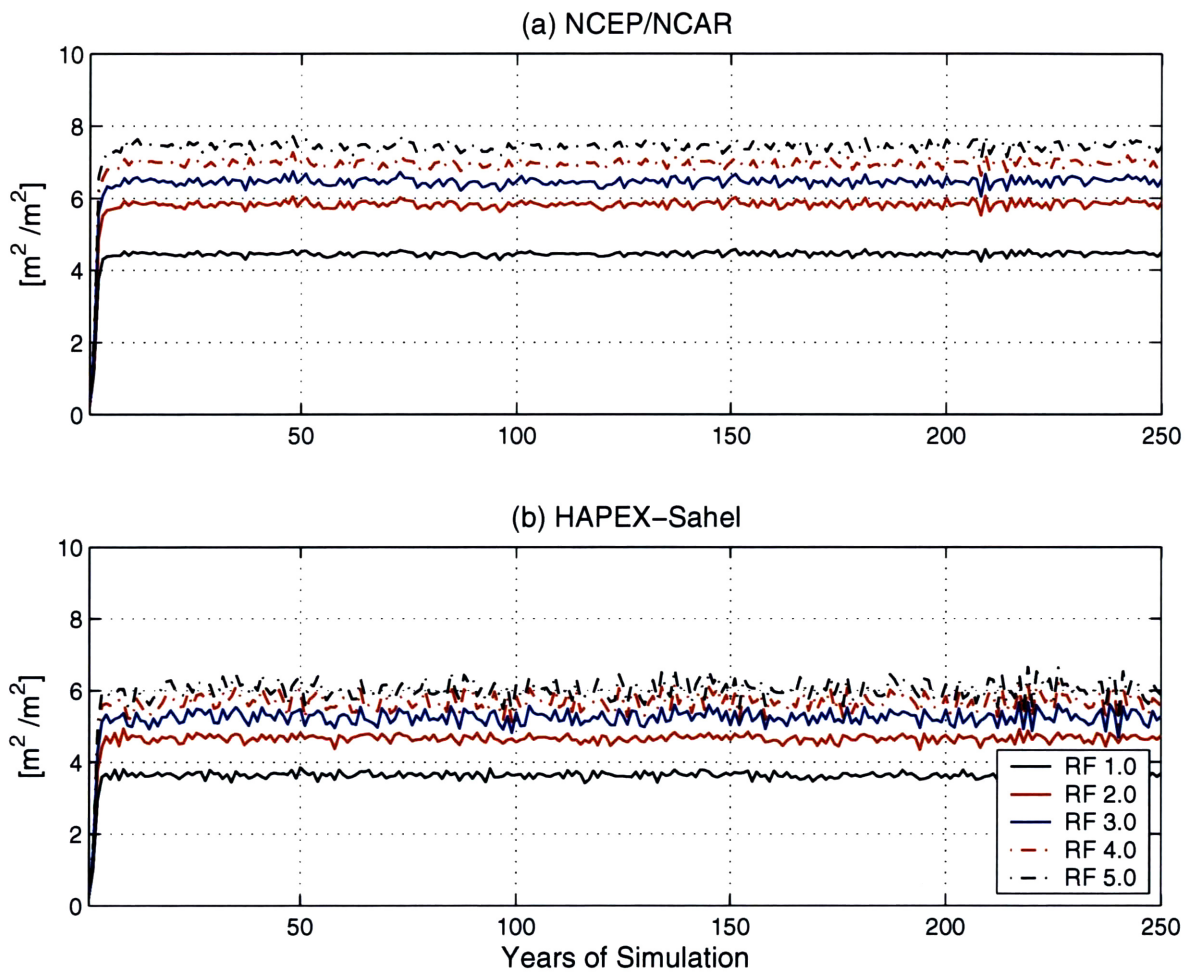


Figure 3-4: Change of the leaf area index (LAI) of the lower canopy during the simulations at 13°N with the data from (a) NCEP/NCAR, and (b) HAPEX-Sahel

same results with the HAPEX-Sahel data, as well. Even with 5 times of the typical rainfall, the model still resolves grasslands as an equilibrium in both (see Figure 3-4).

3.3 Discussion and Conclusion

Our hypothesis is that the variability of topography distributes soil water, which can lead to coexistence of trees and grasses in the same region. To study it, the rainfall variation method is designed. As results suggest, the different types of vegetation are simulated in the regions in 9°N and 11°N, natural savannas. With the simulations in 9°N, tropical deciduous forests are resolved with the normal rainfall, and grasslands with a 30% of rainfall decrease. At 11°N, grasslands with the normal condition, and deciduous forests with a 100% increase of the rainfall input. In the area of 13°N, the model just simulates grasslands regardless of the change of the rainfall inputs. (see Table 3.4)

The hillslope drives the lateral transport of water. Water converges into the concave area through the surface or subsurface runoff. In the dry region, the surface

9°N		11°N		13°N	
RF	Vegetation Type	RF	Vegetation Type	RF	Vegetation Type
1.0	Forest	1.0	Grassland	1.0	Grassland
0.8	Forest	1.3	Grassland	2.0	Grassland
0.7	Forest	1.5	Grassland	3.0	Grassland
0.6	Grassland	1.7	Grassland	4.0	Grassland
0.5	Grassland	2.0	Forest	5.0	Grassland
Savannas		Savannas		Grassland	

Table 3.4: Summarized Results from the Experimental Simulations

runoff occurs often due to the infiltration excess (Hortonian Type), not the saturation excess mechanism (Dunne Type). Furthermore, the West African savannas fall into the tropical climate, where the intense rainfall events are limited in the summer season, and the surface soils may hardly be saturated. In dry hills, the rainfall intensity exceeds the infiltration capacity of the dry soils, then the excess of water in hills converges into wet valleys. Therefore the dry hills and wet valleys coexist in the Sahel region. Under the dominance of Hortonian runoff mechanism, the 40% (in 9°N) and 100% (in 11°N) differences of water between hills and valleys are possible. The simple increase or decrease of available water amounts are enough to create the condition favorable to the different types of plants.

Moreover, simulations of this chapter are performed assuming the soil bottom with a free gravitational drainage condition. This assumption is based on that the region of savannas and grasslands is under the semi-arid climate condition and the details of aquifer condition are not available. As explained in Chapter 2, the model includes only upper soil layers within 4 *m* and defines the soil bottom with a simple coefficient multiplying the unsaturated hydraulic conductivity of the bottom layer, ranging from 0 (no flux) to 1 (free drainage). The more discussion about the lack of groundwater dynamics of the model will be presented in Chapter 5.

Moreover, the models only resolve grasslands as equilibrium ecosystems at 13°N . We observe grasslands in nature. Even with 5 times of the typical rainfall amount, more than 3500 *mm* of the annual accumulated rainfall (based on NCEP/NCAR data), only grasses are simulated in the model. This amount of rainfall is enough to support forests in the areas of 9°N and 11°N . It suggests that the other meteorological

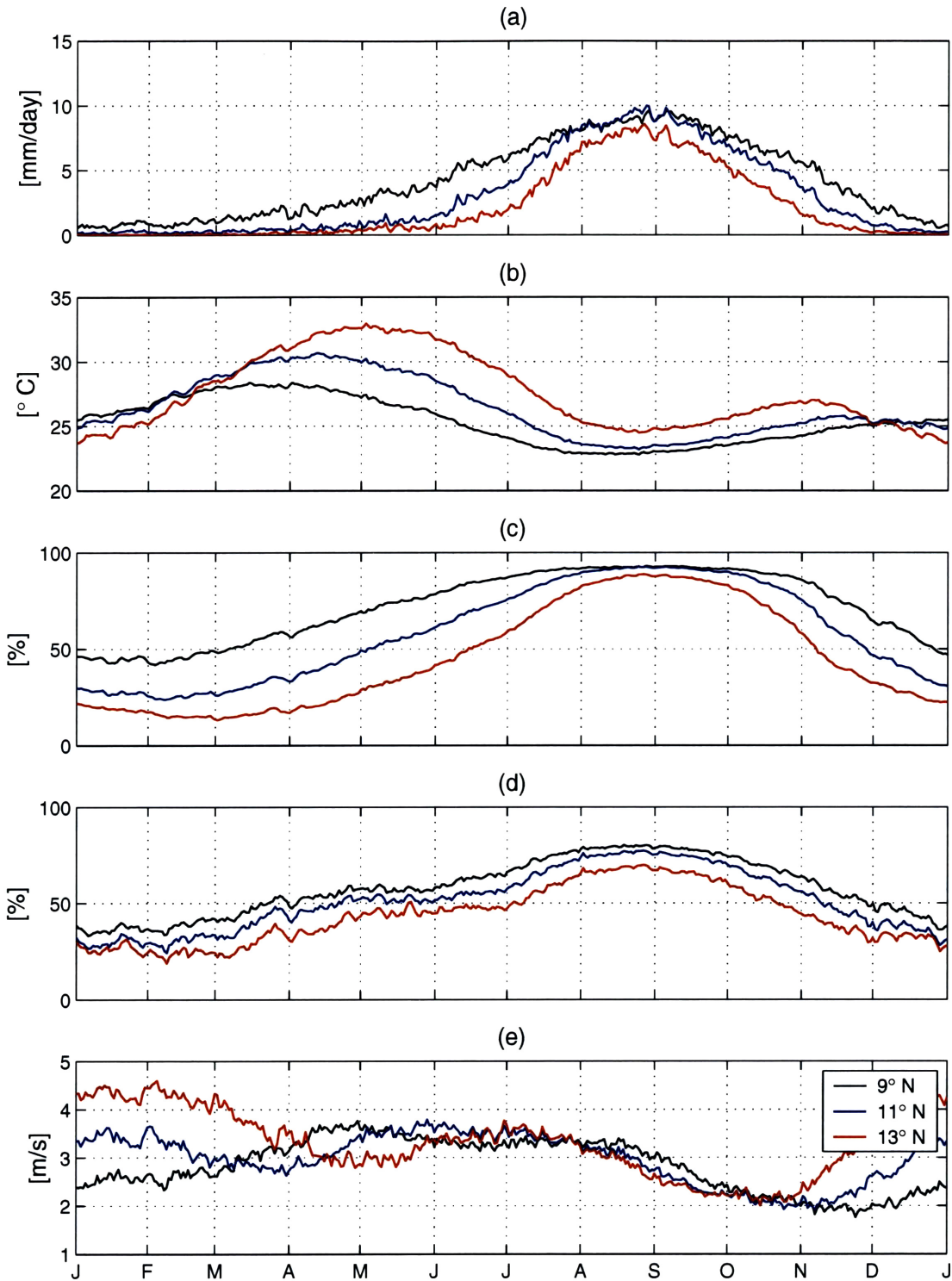


Figure 3-5: Seasonal Cycle of (a) Precipitation, (b) Air Temperature, (c) Relative Humidity, (d) Fractional Cloud Cover, and (e) Wind Speed in 9, 11, and 13°N. This is used as inputs of the model.

conditions may limit this region only as grasslands. Figure 3-5 shows that the area at 13 °N is under more severe environments for plants with higher temperature, less relative humidity, and less cloud cover than others. These perhaps prevent the growth of woody plants.

The models resolve the different types of vegetation in response to the available water only in natural savannas, not in natural grasslands. Under the savanna climate, water is one of the important factors to dictate the vegetation type. Under the climate of grasslands, however, the other environmental factors may limit the growth of trees. Therefore the variability of water availability is important to shape savannas, but it can only play a significant role in the specific climates. In addition, around 1000 *mm* and 2000 *mm* of annual rainfall are required for the transition from grasslands to forests at 9°N and 11°N, respectively. These amounts are quite different although both falls into savannas both in nature and in our experiment. Other meteorological differences perhaps account for this difference. This shows that water is not the only determinant factor of savannas.

To conclude, the results of our experiment show the validity of our hypothesis. But we still need to see how and how much the topographic variation can make soil water different between valleys and hills. Therefore the distributed hydrologic modeling is performed as the next step, which is presented in the following chapter.

Chapter 4

Simulations Using Distributed Hydrologic Model

This chapter presents the simulations using a distributed hydrologic model, SHE, that is described in Chapter 2. The objective is to understand how the variation of topography plays a role in the redistribution of soil water in the environment of savannas in West Africa.

4.1 Details of Simulation

A simulation is performed in a watershed around 13°N in West Africa (see Figure 4-1). To concentrate on the redistribution of soil water in response to the variation of topography in semi-arid climate condition, the model assumes hypothetical conditions such as homogeneous atmospheric condition (daily rainfall and potential evapotranspiration rate) and homogeneous soil properties over its domain.

4.1.1 Study Area

The catchment is situated around 13°N of the Sahel, in the Republic of Niger. The 818.2 km^2 watershed is a part of the area of HAPEX-Sahel as seen in Figure 4-1. Although this area is generally classified as grasslands, we have field data on daily rainfall only for HAPEX-Sahel. For other areas of interest, savannas, we have the climatology of rainfall from the reanalysis project of NCEP/NCAR. The reanalysis data on rainfall shows a less intense and more frequent pattern than field data. The reanalysis data may not be appropriate for distributed hydrologic modeling since it tends to underestimate surface runoff and overestimate infiltration, which are essential processes controlling water movements over a watershed. Hence, we choose to use the available data on rainfall at the area around 13°N to understand the topographic effects redistributing water over land.

4.1.2 Topography

The SHE requires the elevation field over the catchment. GTOPO30 is used here as the source for the elevation data. It is a global digital elevation model (DEM) with a horizontal grid spacing of 30 arc seconds (approximately 1 kilometer), developed by the USGS's EROS Data Center (EDC). To extract a catchment from DEM, the Spatial Analyst and Hydrologic Extension of Arcview are used.

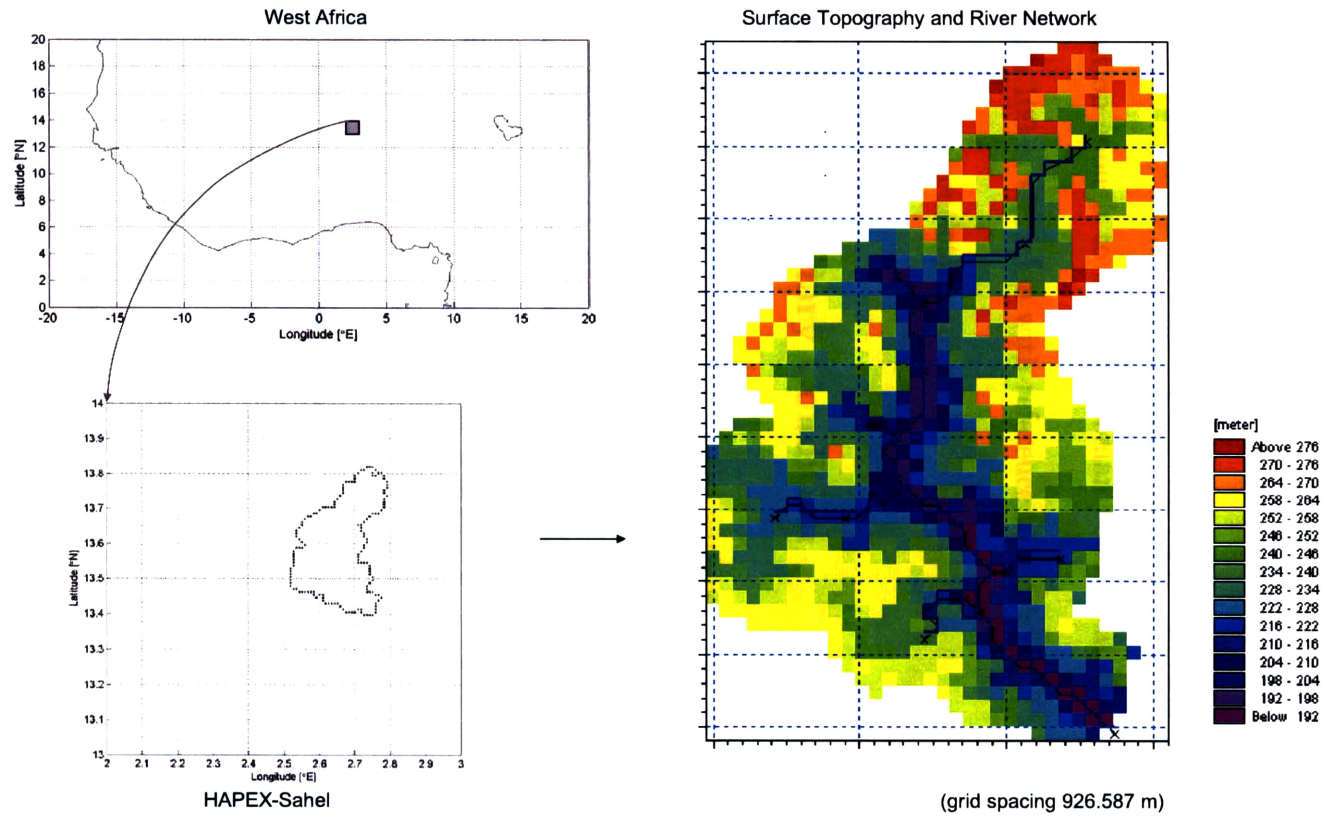


Figure 4-1: The Study Area

4.1.3 Soil Profile

Soil is discretized with uniform thickness laterally by the ground surface as the reference (see Figure 4-2). Soil is discretized with 10 *cm* above 1 *m* depth, 20 *cm* between 1 and 11 *m* depth, 50 *cm* below 11 *m* depth. The upper part of soil is discretized with a fine resolution enough to allow Hortonian ponding at the land surface. Soil bottom is flat with 100 *m* elevation with reference to sea level. The lowest elevation in a watershed (a channel outlet) is 188 *m*.

4.1.4 Initial and Boundary Condition

Initially, the water table is assumed to be at the surface. The daily time series of a year is used for the atmospheric conditions, and is repeated until the hydrologic variables, such as depth to water table, reaches equilibrium regardless of the initial arbitrary conditions. By monitoring the fluctuations of water table, we know the model approaches the steady state when it does not show significant yearly changes. The simulations were run for 60 years, which was enough for the model to reach steady state.

In addition, the catchment has no flow through the lateral boundary and bottom boundary. The outflow from the domain takes place only through the channel discharge point at the outlet.

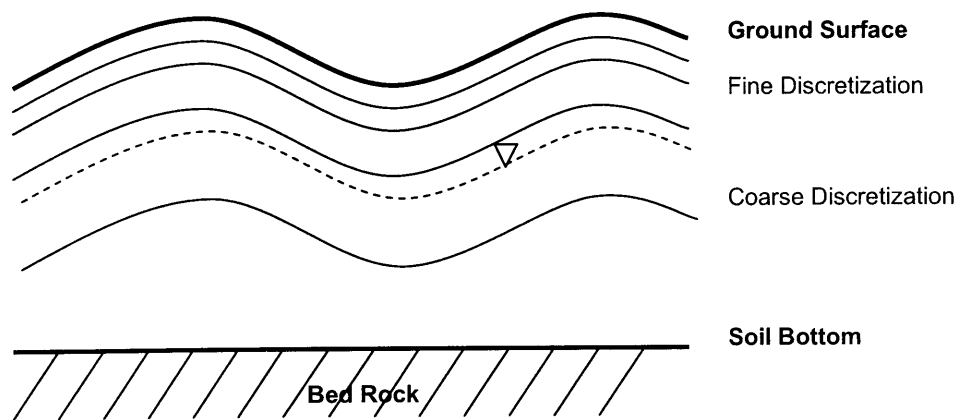


Figure 4-2: Soil Discretization

4.1.5 Atmospheric Forcings

As atmospheric boundary conditions, rainfall rate and potential evapotranspiration are needed to run the model. Rainfall data is taken from the field data of HAPEX-Sahel (Goutorbe, 1997). Rainfall is measured with the EPSAT-Niger (Estimation des Pluies par Satellite) network of 107 recording rain gauges in HAPEX-Sahel. 34 rain gauges are included in the delineated catchment, and their rainfall data are averaged in space for the simulation. To get the daily potential evaporation rate, IBIS (Integrated Biosphere Simulator) is run using rainfall of HAPEX-Sahel and other atmospheric conditions (air temperature, relative humidity, fraction of cloud cover, and wind speed) of NCEP/NCAR reanalysis project. In IBIS, a fully saturated bare soil is assumed during this simulation, and the resulting evaporation is assumed to be the potential evaporation rate.

4.1.6 Soil Property

The soil is assumed to be homogeneous and isotropic bare soil over the whole watershed. The soil properties used are the typical values for loamy sand (Rawls *et al.*, 1992; Freeze & Cherry, 1979). For the saturated zone, the hydraulic conductivity of $7.2 \text{ e-}06 \text{ m/s}$ and specific yield of 0.1 are assumed.

The SHE describes the unsaturated flow using the one-dimensional Richards equation, requiring two hydraulic functions, the moisture retention curve and the hydraulic conductivity curve. The van Genuchten model is applied to describe the retention

curve:

$$\theta(\psi) = \theta_r + \frac{(\theta_s - \theta_r)}{[1 + (\alpha\psi)^n]^m} \quad (4.1)$$

and the Averjanov formula is used to describe the hydraulic conductivity curve:

$$K(\theta) = K_{sat} \left(\frac{\theta - \theta_r}{\theta_s - \theta_r} \right)^N \quad (4.2)$$

where α is the inverse of the air entry value, n and m are shape parameters of the van Genuchten relation, and N is the shape parameter of Averjanov model. The following tables show the assumed values for the loamy sand soil.

Variable	Value
θ_s [-]	0.391
θ_r [-]	0.049
α [1/cm]	0.032
n [-]	1.76
m [-]	0.4318
N [-]	5.6316

Table 4.1: Soil Parameters for Unsaturated Zone

4.2 Results and Analyses

The distribution of soil moisture is influenced by the topographic characteristics such as the relative elevation and shapes of hillslope. Water converges into relatively low, concave area of hillslope by the lateral transport of water. To relate the simulated

hydrologic variables with the topography, in addition to elevation, the curvature (C) of hillslope are calculated with the laplacian of the elevation (z) as the following:

$$C = \nabla^2 z = \frac{\partial}{\partial x} \left(\frac{\partial z}{\partial x} \right) + \frac{\partial}{\partial y} \left(\frac{\partial z}{\partial y} \right) \quad (4.3)$$

where x and y is rectangular Cartesian coordinates. The valleys have the positive curvature (concave) and hills have the negative curvature (convex). The first figures of Figure 4-3 and 4-4 show the elevation and its curvature, respectively.

To understand the influence of topography on the spatial distribution of soil moisture, the water content of top 1 m soil is calculated for each month. Figure 4-3 and 4-4 show that more soil moisture is detected in the area, having relatively low elevation and concave shapes of hillslope. To quantify it, the correlations between elevation and soil moisture, and curvature and soil moisture are analyzed. As seen in Figure 4-5, the correlation coefficient between the elevation and soil water is around 0.38, and that between curvature and soil moisture is around 0.67. Both have the maximum in September. The curvature is more correlated with soil moisture than the elevation. In other words, the shapes of hillslope are relatively dominant control factor although the relative elevation and shape of slopes have combined effects on the heterogeneity of soil water.

Now, the question moves into which hydrologic processes make the influences of topography (mainly by shape of hillslope) exert the variability of soil moisture. In general, relatively low, concave area can have more water due to shallow water table or the surface runoff from concave area of hillslope. Thus two hydrologic variables of

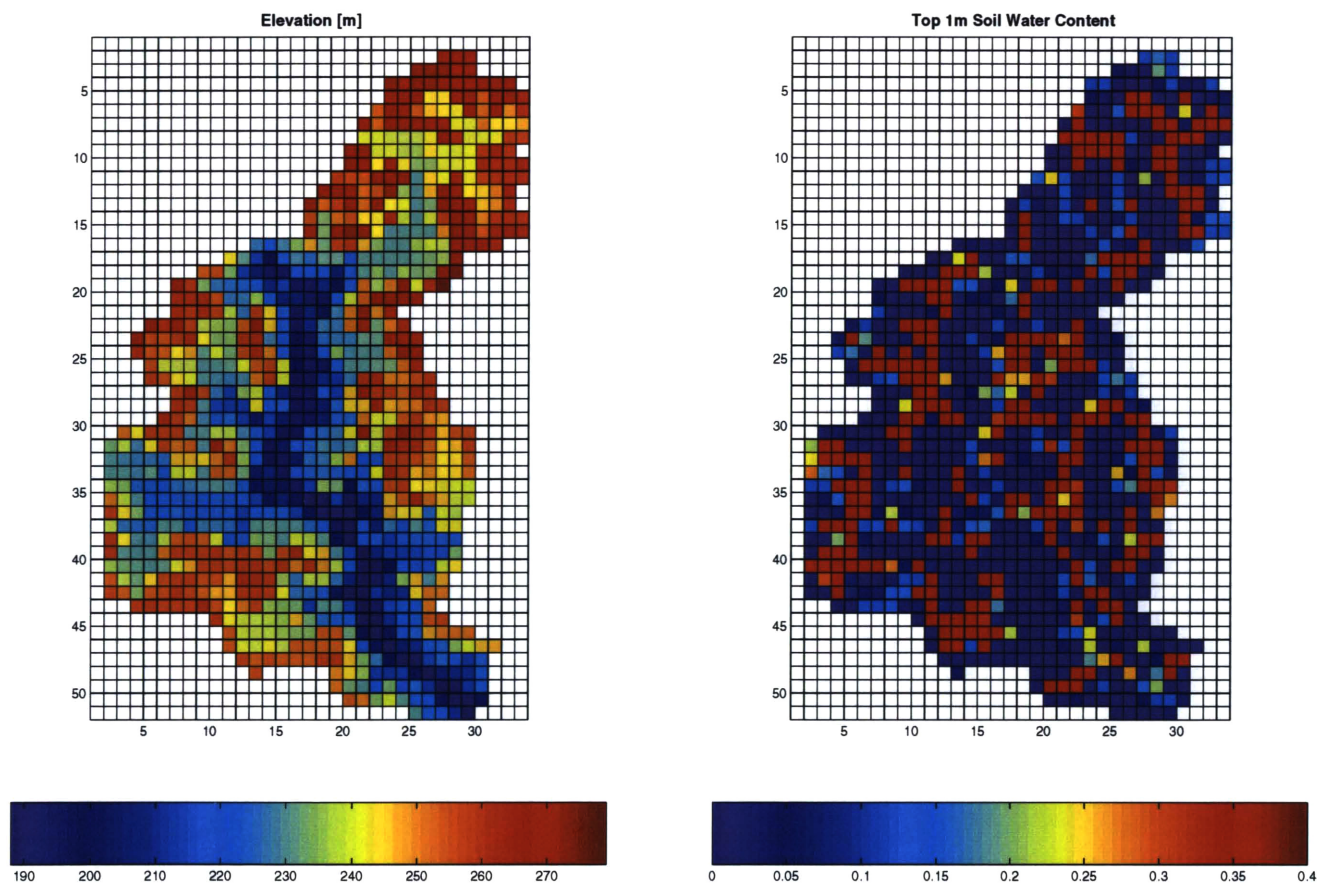


Figure 4-3: Topography and Simulated Soil Moisture of August

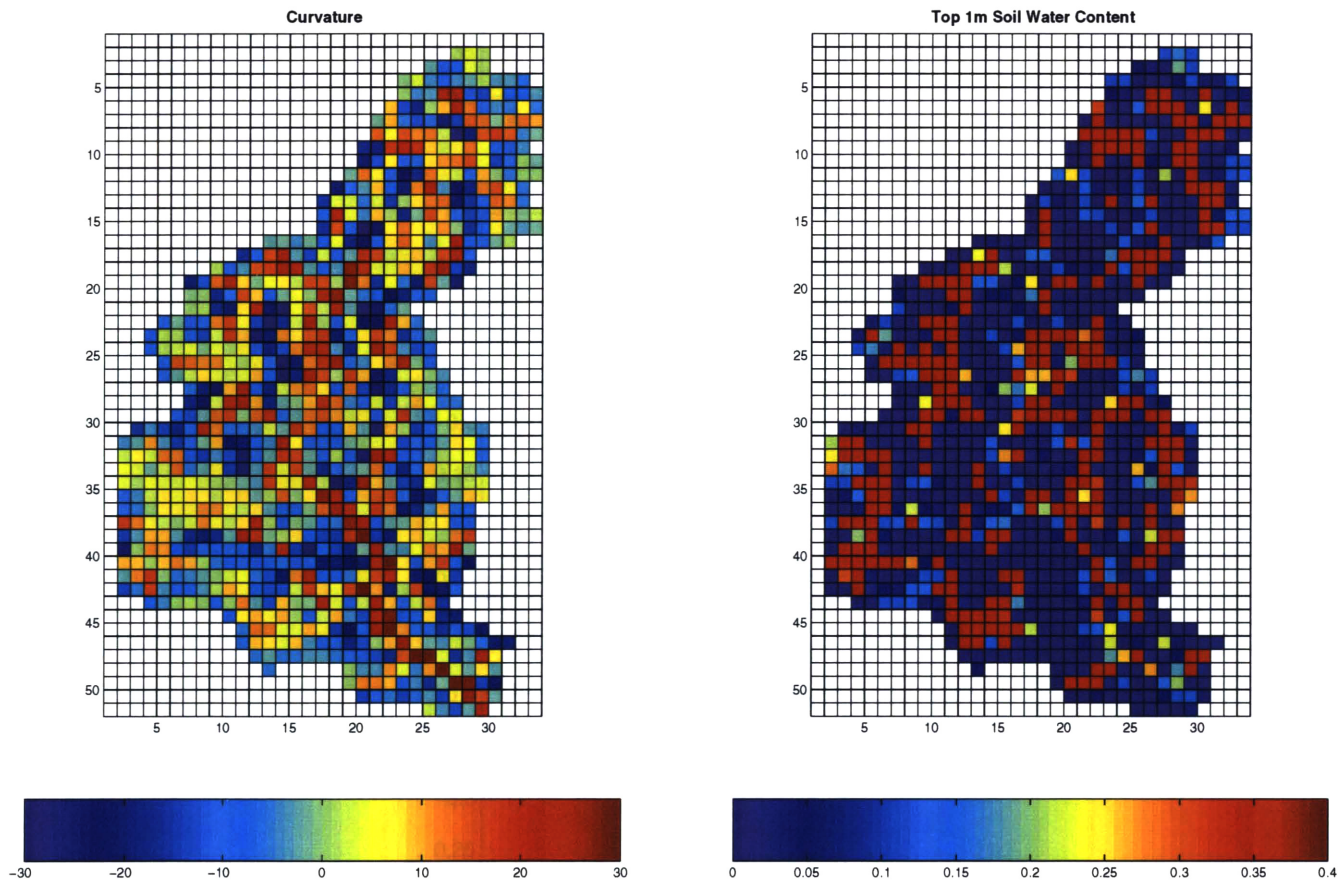


Figure 4-4: Curvature and Simulated Soil Moisture of August

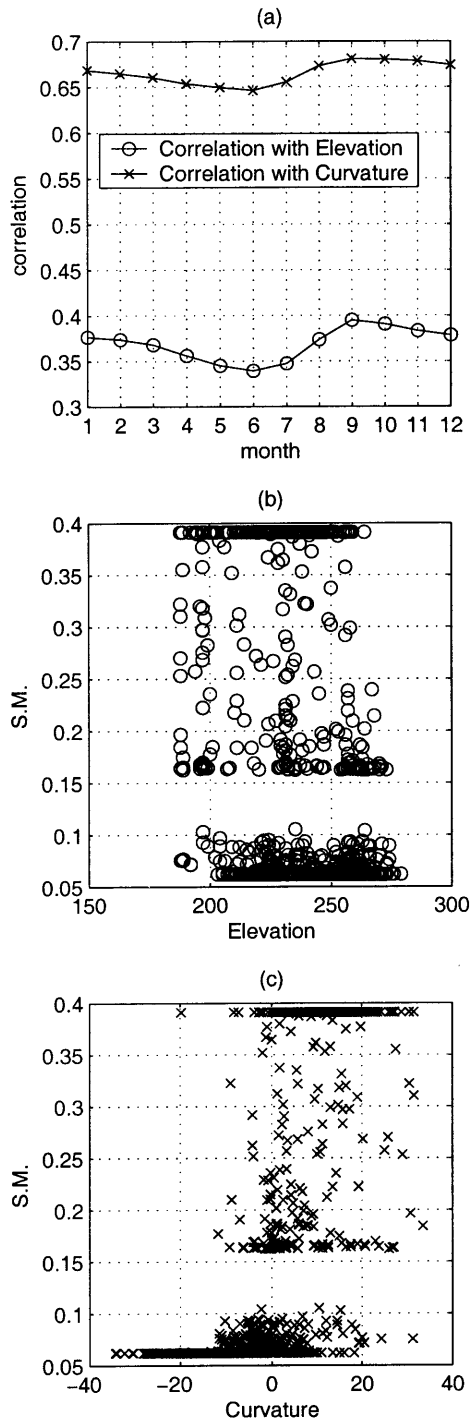


Figure 4-5: (a) Monthly correlations between elevation and top 1m soil moisture, and between curvature and top 1m soil moisture, (b) Elevation and top 1m soil moisture in August, and (c) Curvature and top 1m soil moisture in August

the depth to water table and surface lateral flow are of interest now.

4.2.1 Influences of Depth to Water Table

The simulated water table depth and soil moisture in top 1 *m* soil are presented in Figure 4-6. The area having shallow water table and more soil moisture is indicated by the red color. Their distribution is similar, and it suggests that wet soil water conditions are associated with the area with the shallow water table. The correlation between soil moisture and water table depth is analyzed in case water table depth is shallower than 8 *m*. Figure 4-7 (a) shows significant correlation coefficient throughout a year. The variability of soil moisture depends on the depth to water table, and their relation is well defined as shown in Figure 4-7 (b).

In the above, it is noted that the shape of hillslope plays a significant role in the redistribution of soil water. Therefore, the curvature can represent the topographic effects. A scatter plot with the convexity and water table depth (see Figure 4-7 (c)) shows a clear relationship between them, suggesting that the topography apparently influences the soil water variability through the variation of water table depth.

4.2.2 Influences of Surface Lateral Flow

The surface lateral outflow (*O*) from a grid is calculated from the output variables by

$$\bar{O} = \bar{P} - \bar{I} - \bar{E}_{pw} \quad (4.4)$$

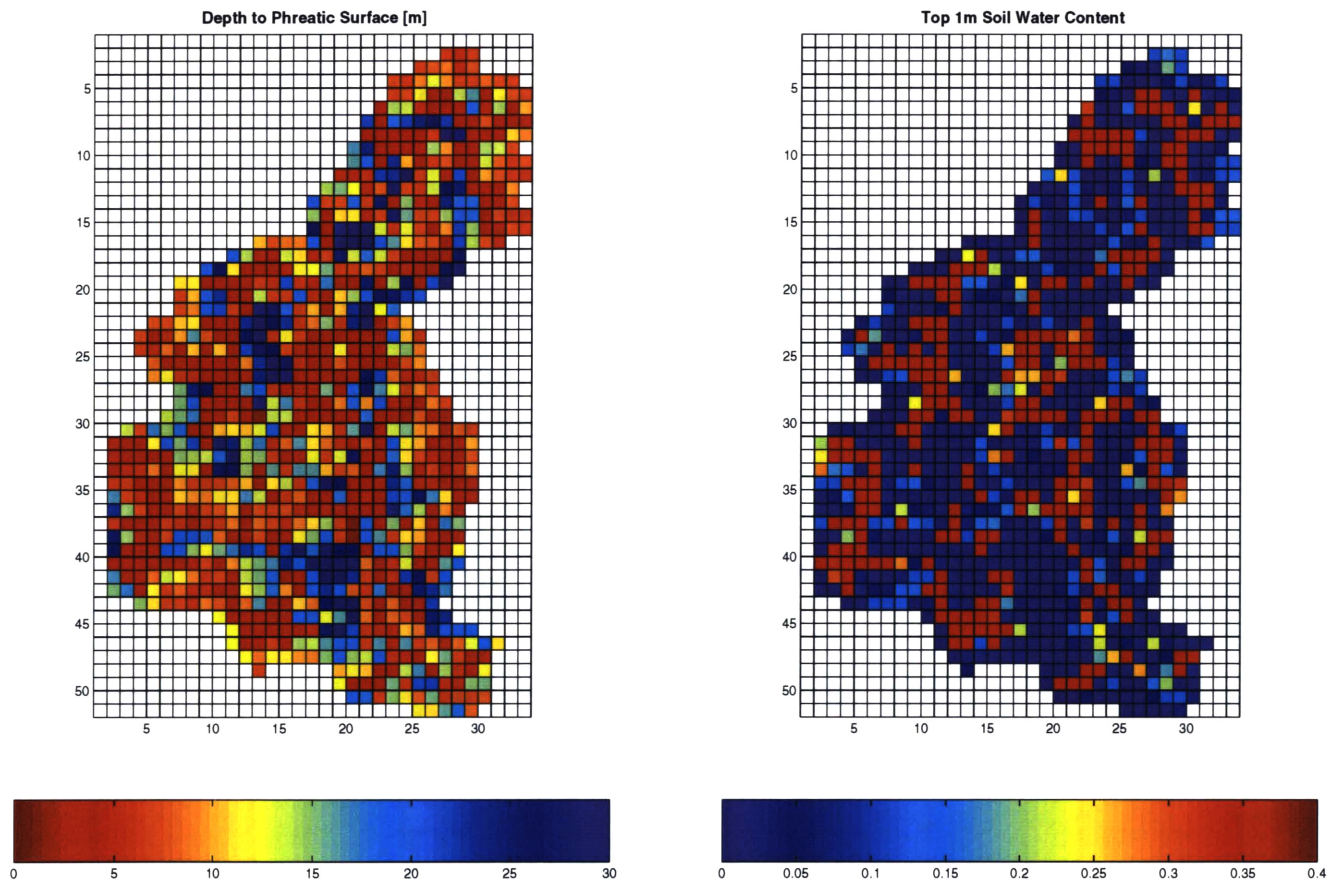


Figure 4-6: Simulated Depth to Water Table and Soil Moisture of August

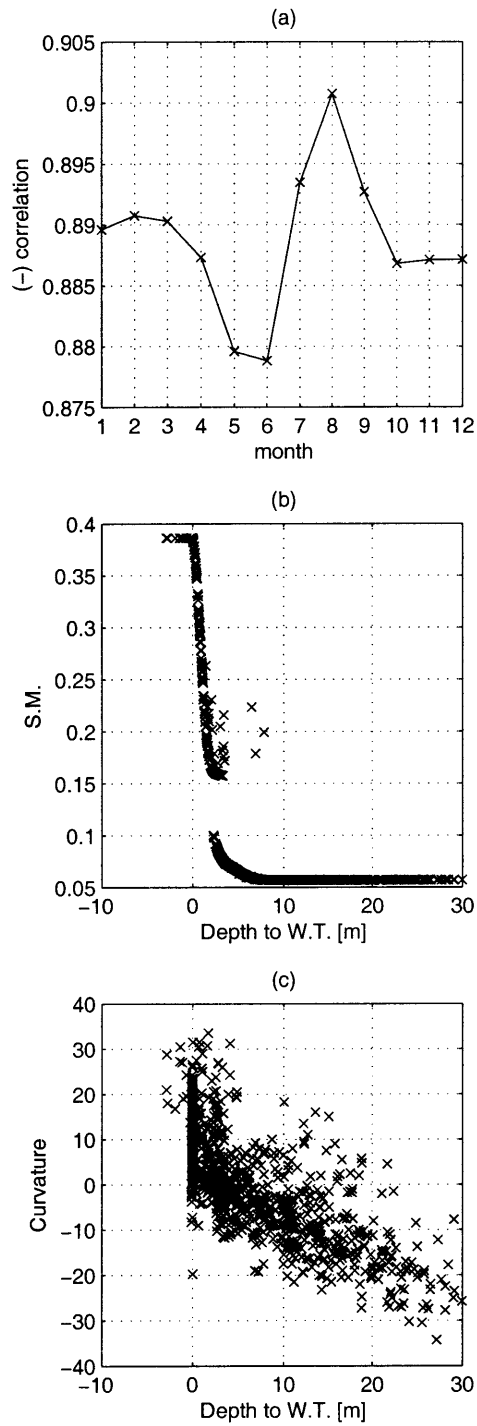


Figure 4-7: (a) Monthly correlations between water table depth and top 1m soil moisture, (b) top 1m soil moisture and water table depth in August, and (c) Curvature and water table depth in August

where P is the rainfall rate, I is the infiltration rate, and E_{pw} is the evaporation rate from ponded water. The overbar means the mean value, and the monthly mean is calculated here.

During the rainy season, both the surface lateral inflow and outflow usually take place on the valley area, and outflow is generated in the more wet area of valleys (see Figure 4-8 and 4-9). However, if the redistribution of water is significantly prompted by the surface flow from hills to valleys, we might see the negative correlation coefficients during or after the intense storm. It implies that hill areas do not produce the significant amount of surface runoff. Therefore the surface lateral flow does not significantly affect the variation of soil moisture between hills and valleys.

4.3 Conclusion

The distributed hydrologic modeling is performed over the semi-arid region around 13°N, in order to see the effects of topography on the heterogeneity of soil water. Apparently, the spatial distribution of soil water is dictated by the topographic characteristics such as the shape of slope and relative elevation. The shape of hillslope are relatively important, which can lead to the soil water variability through the water table depth.

The depth to water table is suggested as a significant hydrologic variable in spatial distribution of soil moisture in Sahel of West Africa. As noted in Chapter 3, the water availability is important for the coexistence of trees and grasses in savannas. Therefore the variation of water table can play a significant role in shaping savannas, which will

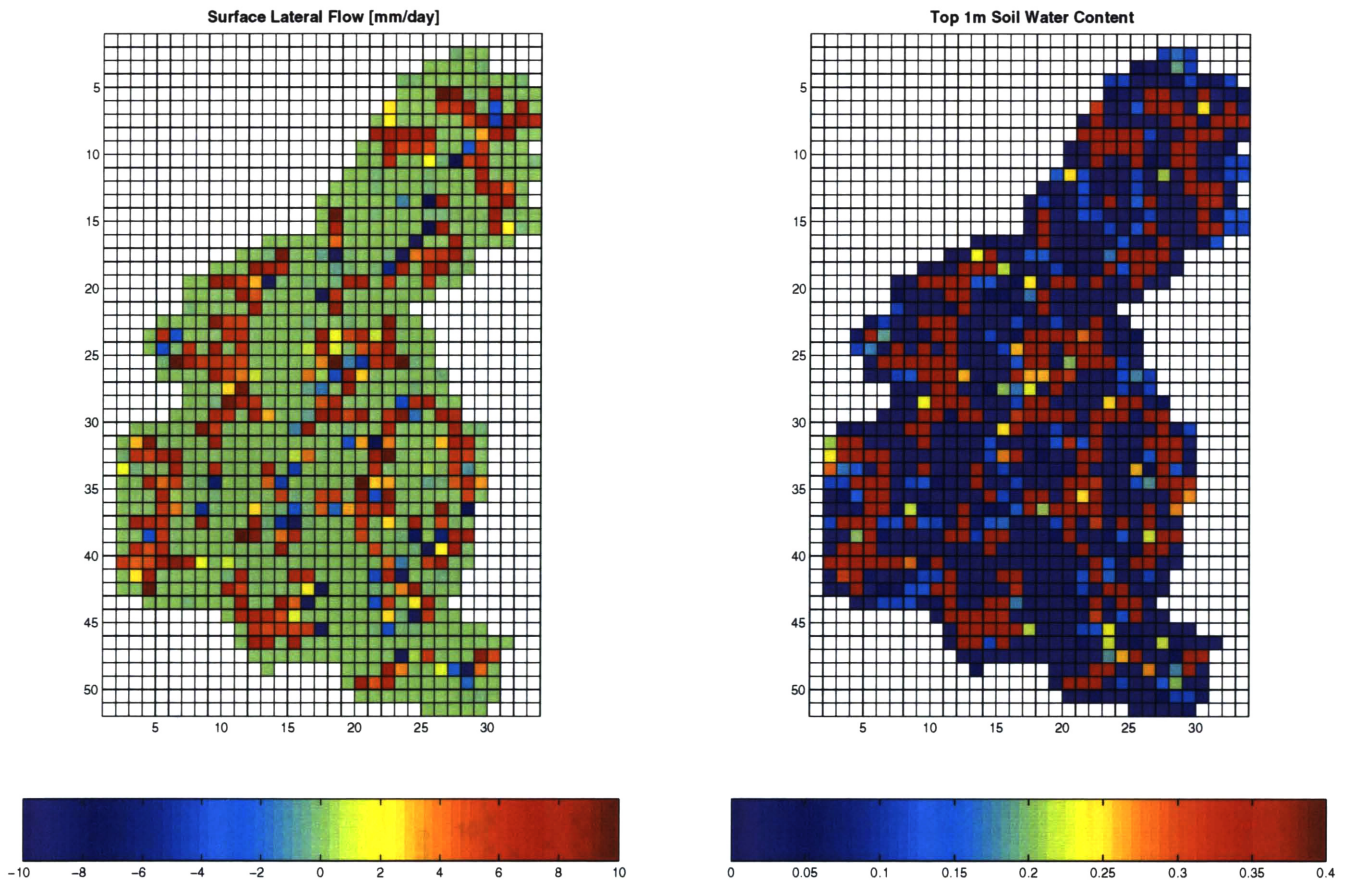


Figure 4-8: Simulated Surface Lateral Flow and Soil Moisture of August

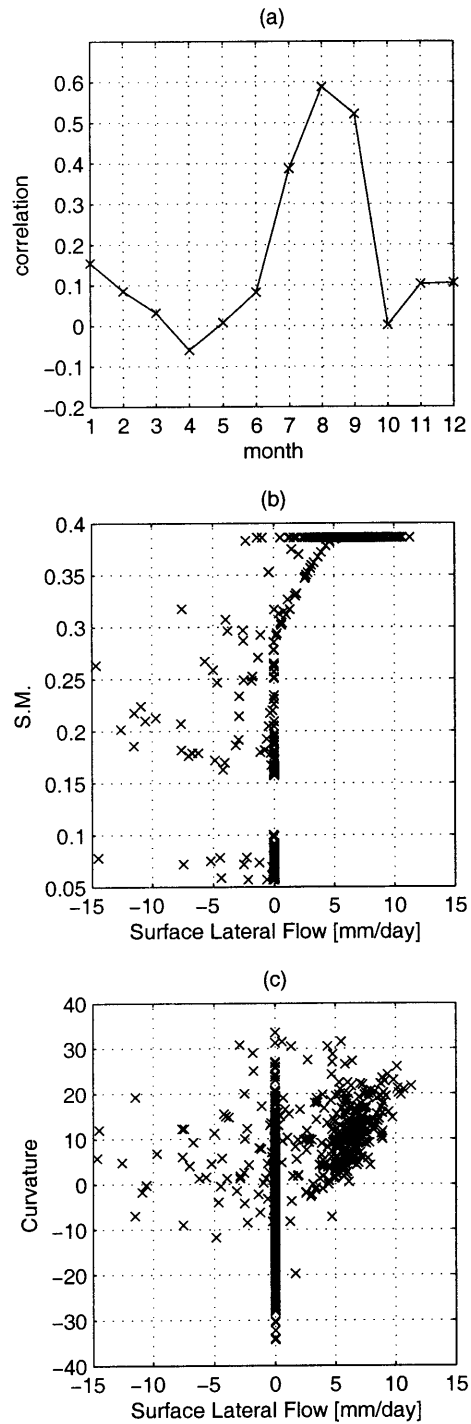


Figure 4-9: (a) Monthly correlations between surface lateral and top 1m soil moisture, (b) top 1m soil moisture and surface lateral flow in August, and (c) Curvature and surface lateral flow in August

be studied in the next chapter.

Chapter 5

Simulations Using IBIS and Including Groundwater Table

The hypothesis of Chapter 1 is tested in this chapter, using the modified IBIS. The soil model of IBIS is modified to include the groundwater table depth as a boundary variable, which facilitates a coupling of IBIS and SHE asynchronously. The different mean water table depths over the watershed, which resulted from the SHE simulations, reflect the spatial variability of elevation that has been suggested to explain the coexistence of trees and grasses in the hypothesis of Chapter 1.

5.1 Asynchronous Coupling of IBIS and SHE

The distributed hydrologic modeling of Chapter 4 suggests that the water table depth is highly correlated with soil moisture. The variation of soil moisture can dictate the different types of vegetation, trees and grasses, given the climate of savannas as

presented in Chapter 3. Consequently, it is expected that the spatial variability of water table depth can lead to the coexistence of trees and grasses in a region. The shallow water table supplies more water to soil and vegetation than the deep one. Different water table depths provide the soil with different amounts of water, the source of evapotranspiration, and hence the soil can support the different types of vegetation. Using IBIS, however, this cannot be tested in a direct way, since the model does not represent the groundwater table.

The current LSX (Pollard & Thompson, 1995; Thompson & Pollard, 1995a; Thompson & Pollard, 1995b), used in the IBIS for the land surface processes, does not represent the dynamics of water table physically. In the LSX, the bottom boundary condition of soil is specified as the unsaturated conductivity of the lowest layer multiplied by an empirical drainage coefficient ranging from 0 to 1. 0 is no flux condition such as impermeable bedrock, and 1 is gravity drainage condition. Since the coefficient control the drainage rate out of the soil column, it has an important impact on partitioning between the runoff and evapotranspiration. However it is impossible to estimate the coefficient in the field since it is not physically based, and is rather ambiguous. Including the LSX, the most current models do not include the water table since the large grid scale and thin soil layers of soil column make the groundwater dynamics a seemingly insignificant hydrologic process in the models (Yeh, 2003). Therefore the land surface models apply a gravitational drainage condition or linear function of gravity drainage condition with an empirical coefficient which accounts other factors affecting soil drainage such as the topographic slope and amplitude, or the location of bed rocks (Boone & Wetzel, 1996).

Since it is difficult to include the groundwater dynamics in the land surface model, we specify the groundwater table as a boundary variable, instead of including a physically-based groundwater model. From the results of SHE, we can take the annual cycle of groundwater table, which is at the different grid cells of the distributed model. Valley areas have shallow water table depth, and are sensitive to the storm events. Hill areas have deep water table depth, and are less sensitive to the storm events than valley areas. Therefore, the bottom boundary of IBIS can be specified according to the cycle of groundwater table at the different topographic characteristics. Then, we expect that the biospheric model should show the different equilibrium vegetations of tree or grass, according to the soil bottom condition specified with the water table level (see Figure 5-1). To include the groundwater table as a boundary, the soil model of IBIS is modified, and the modification is described in the next section.

5.2 Modification of IBIS

IBIS is modified to include the groundwater table depth as a boundary variable. In the soil model of IBIS, the multilayer model is used to simulate soil water in the upper soils. Water diffuses and drains with nonlinear dependence on soil water according to the following:

$$\begin{aligned}
 n \frac{\partial w}{\partial t} &= \frac{\partial}{\partial z} \left(K(w) + D(w) \frac{\partial w}{\partial z} \right) \\
 &= \frac{\partial}{\partial z} \left(K_s w^{2B+3} - K_s \psi_s B w^{B+2} \frac{\partial w}{\partial z} \right)
 \end{aligned}
 \tag{5.1}$$

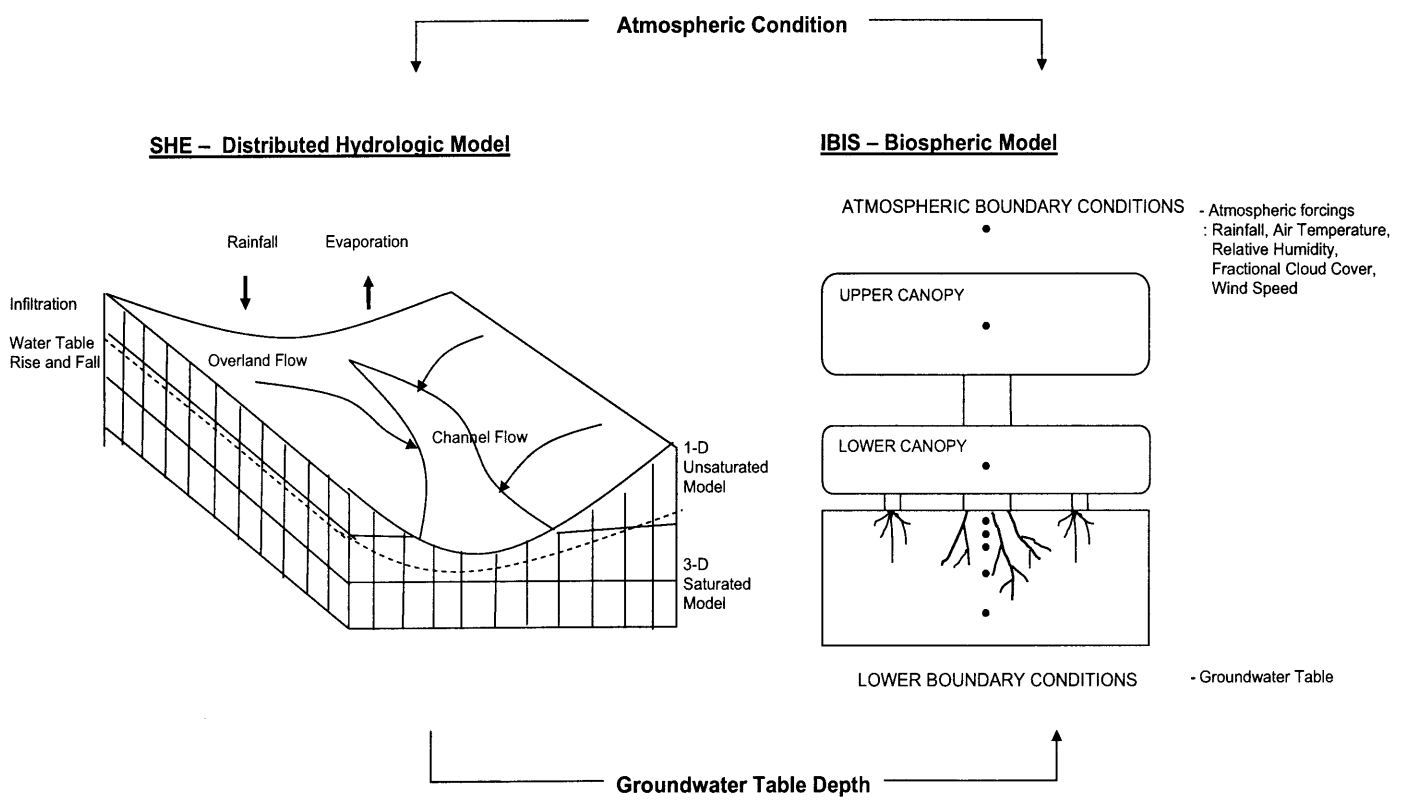


Figure 5-1: Asynchronous Coupling IBIS and SHE

where n is the soil porosity, w is fractional liquid water content (saturation degree), K_s is the saturated hydraulic conductivity, ψ_s is the saturated matric potential, B is an empirical soil exponent, $K(w)$ is the hydraulic conductivity depending on soil water, and $D(w)$ is the diffusion coefficient depending on soil water. The empirical relations to estimate the unsaturated hydraulic conductivity and tension (Brooks & Corey, 1966) are applied to the Richards equation. The first term on the right-hand side is the drainage rate (unsaturated hydraulic conductivity) due to gravity, and the second term is diffusion.

In practice, the soil columns are discretized with N sub-layers. In the finite difference method, the boundary of unsaturated model, the $(N + 1)th$ layer only have a gravitational drainage controlled by the drainage coefficient (C), which is

$$\text{Drainage Rate} = K(w) \cdot C = (K_s w^{2B+3}) \cdot C \quad (5.2a)$$

$$D = 0 \quad (5.2b)$$

where w is the saturation degree of Nth layer, C is ranging from 0 to 1.

Yeh (2003) modified the soil model of IBIS to represent the dynamics of groundwater table. The modified model simulates the change of groundwater table depth with the nonlinear groundwater runoff function under two estimated parameters. However, in this study, the part of modified soil model is adapted to simulate the movement of soil moisture under the given groundwater table. The modified model runs the unsaturated soil model of Eq. 5.1 up to the water table. The given water table depth

provides the number of unsaturated layers (M). Hence, $(M + 1)th$ layer has the gravitational drainage and diffusion term both with w of 1. Thus the $(M + 1)th$ layer has the drainage rate (saturated hydraulic conductivity) and diffusion coefficient (D) as the followings:

$$K(w = 1) = K_s \tag{5.3a}$$

$$D(w = 1) = -K_s \psi_s B \tag{5.3b}$$

The discretization of soil must be fine enough to capture the given change in the depth of unsaturated zone. In this study, the soil profile is the same with the soil profile of hydrologic modeling of Chapter 4.

5.3 Details of Simulation

The area of interest is the same as that in the former experiments with IBIS of Chapter 3. The region of 9°N and 11°N are savannas, which is to test the hypothesis of savanna existence, and the region of 13°N is grasslands where the model should not result in savannas.

First, to get a boundary condition of IBIS, we simulate using the SHE in the three regions of 9, 11, and 13°N. The SHE simulation at 13°N with HAPEX-Sahel field data is already performed, as presented in Chapter 4. We do the same simulations in other regions, just changing the atmospheric conditions (rainfall and potential evaporation rate). Although in reality the topography is different according to the region, we use

the same watershed for all cases. Although this may not be realistic, the objective is to test if the variability of water table depth can result in the coexistence of trees and grasses, not to reproduce the real situation. Moreover, we can compare the response of watershed according to the different amounts of available water at the different latitude.

Then we run IBIS with the annual cycle of daily water table depth, expecting the area of the shallow (deep) water table might have trees (grasses) as an equilibrium in natural savannas such as the region of 9 and 11°N.

It is noted that the region of 9°N is not included in this experiment. The soil bottom is assumed with the free gravitational drainage condition in Chapter 3 since we do not know the exact aquifer condition and West Africa is known as a semi-arid region. Therefore putting water table in the model acts as adding water for soils in this study. Moreover, at 9°N, the model simulates forests under the free gravitational drainage condition, and we get a transition from forests to grasslands as we decrease the amount of rainfall input in Chapter 3. We expect to get trees regardless of water table depth, since by adding a groundwater table we can only make the soil condition more wet, compared to the former simulations of IBIS.

5.4 Results

5.4.1 Experimental Simulation 1: 11°N

Figure 5-2 presents the annual mean water table depth, while showing the different topographical areas have different mean depth. Moreover, as the water table depth gets shallow, it gets sensitive to the atmospheric forcings (see Figure 5-3).

At 11°N, the biospheric model simulates grasslands under the normal condition. We expect the shallow water table might allow trees over a region, and we try to find the transition from trees to grasses (see Figure 5-4 and 5-5).

With the daily annual water table depth of location A, grasslands are simulated. The lower canopy LAI of location A stays around 6.5, and upper canopy LAI is quite small, approximate less than 0.2. On the other hand, in the location B, the upper canopy LAI become around 3 after 350 years. The location B is dominated by trees, it is a deciduous tropical forest. If the mean water table depth is shallower than 2.6 *m* (mean water table depth of location A), the grid cells of hydrologic modeling would have trees. Then we calculate the fraction of trees according to the annual mean water table depth of Figure 5-2, about 8% of watershed area are dominated by trees.

5.4.2 Experimental Simulation 2: 13°N

At 13°N, the model simulates grasslands under the normal atmospheric condition with the assumption of free drainage condition of soil bottom. In nature, this area consists of grasslands. Therefore the shallow water table depth would not allow the model to simulate the trees if the area is grasslands, based on the experimental design.

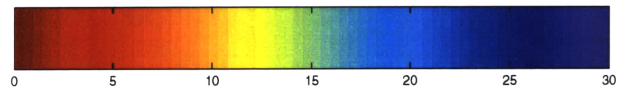
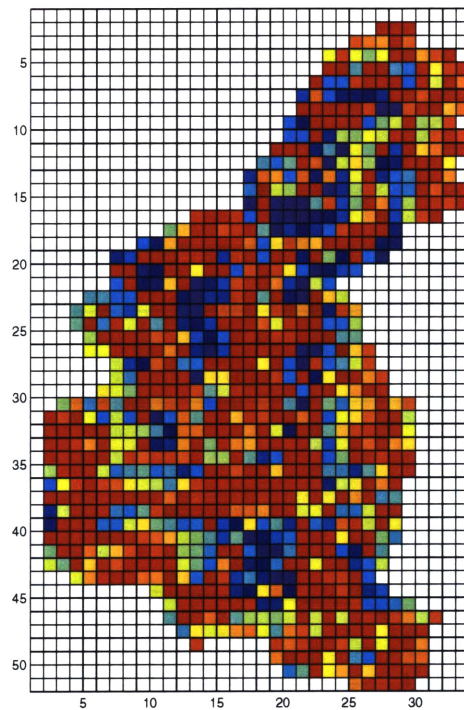


Figure 5-2: Simulated Mean Water Table Depth of 11°N

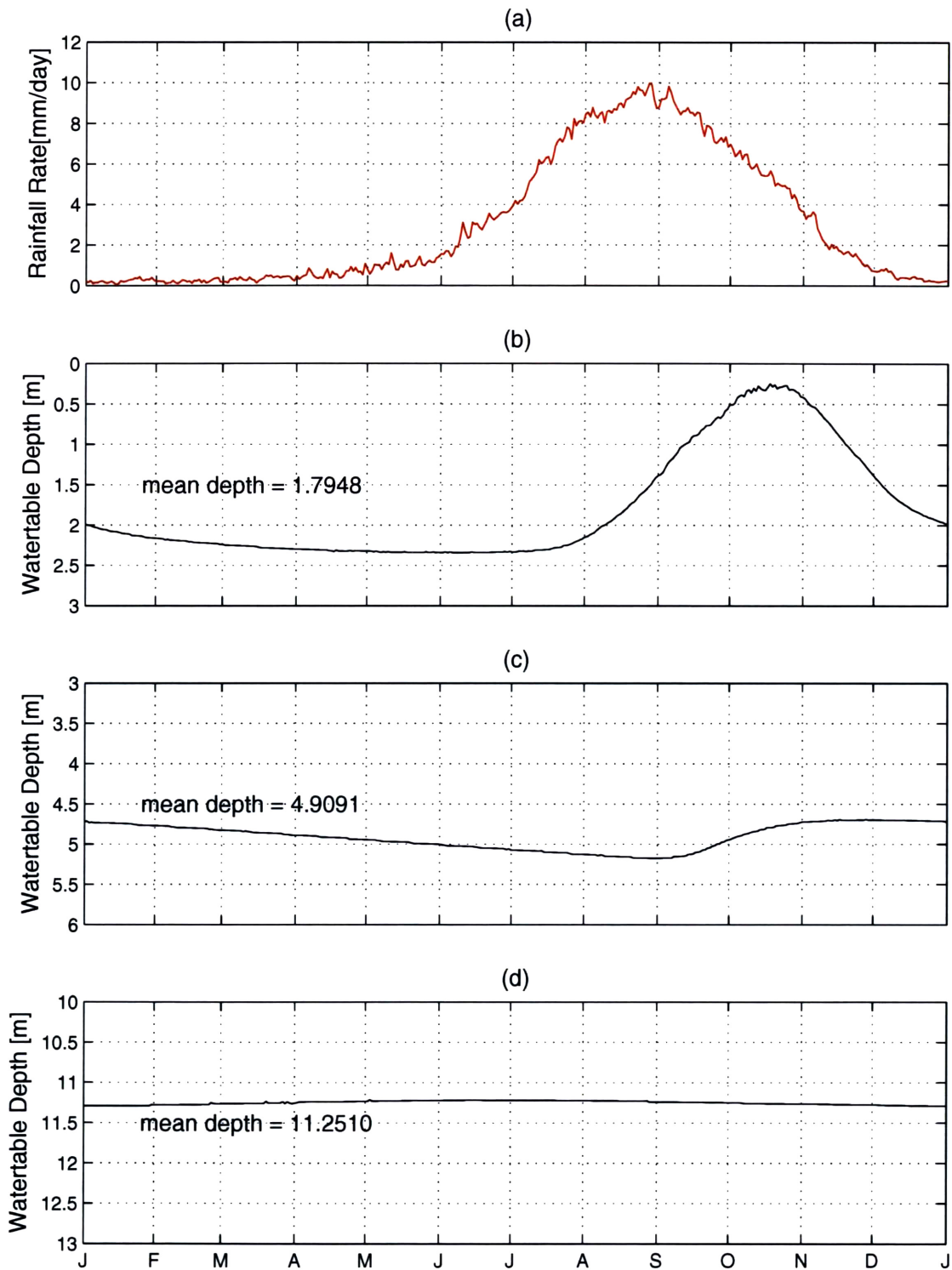


Figure 5-3: Annual Cycle of (a) Rainfall Rate, and (b), (c) and (d) Groundwater Table Depth of Different Means in 11 °N

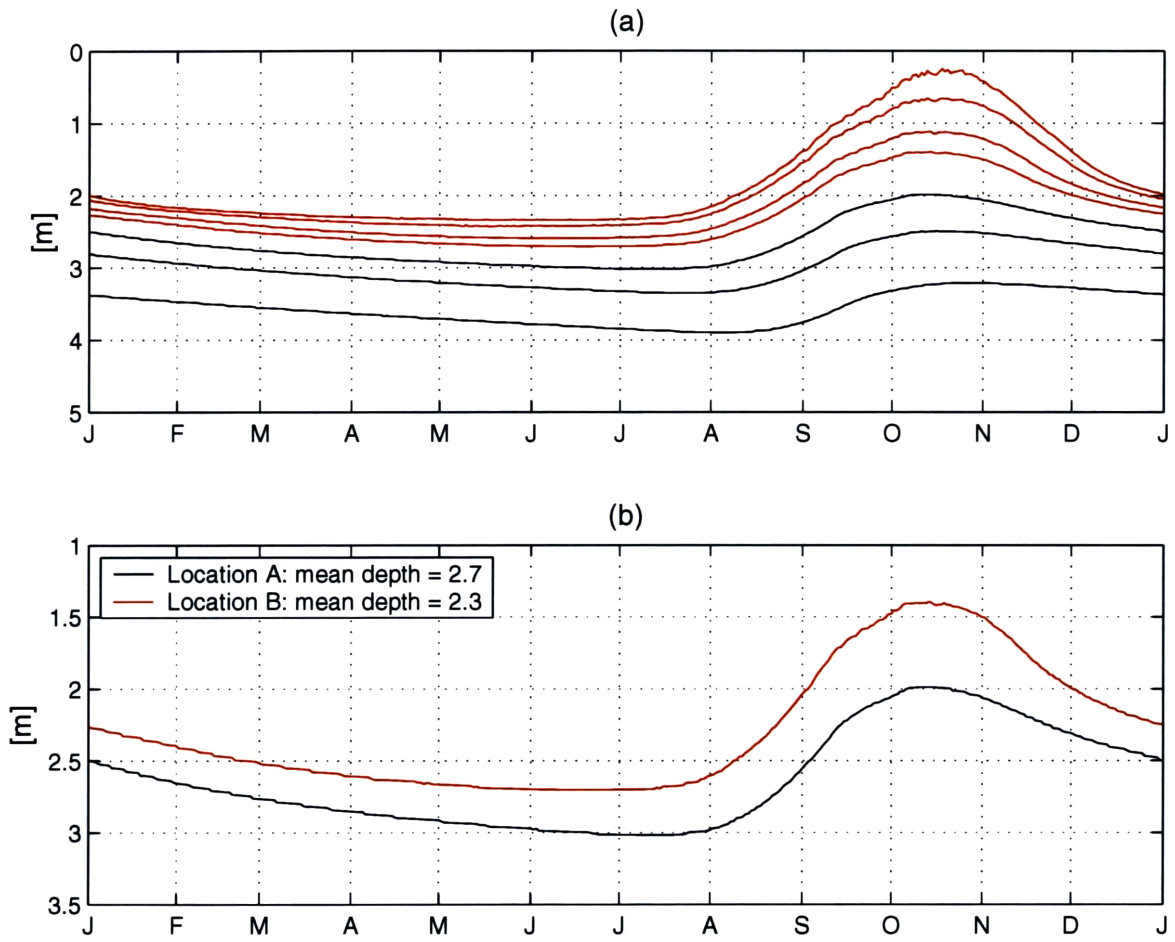


Figure 5-4: Annual Cycle of Groundwater Table Depth, Simulating Trees (Red) and Grasses (Black) at 11 °N

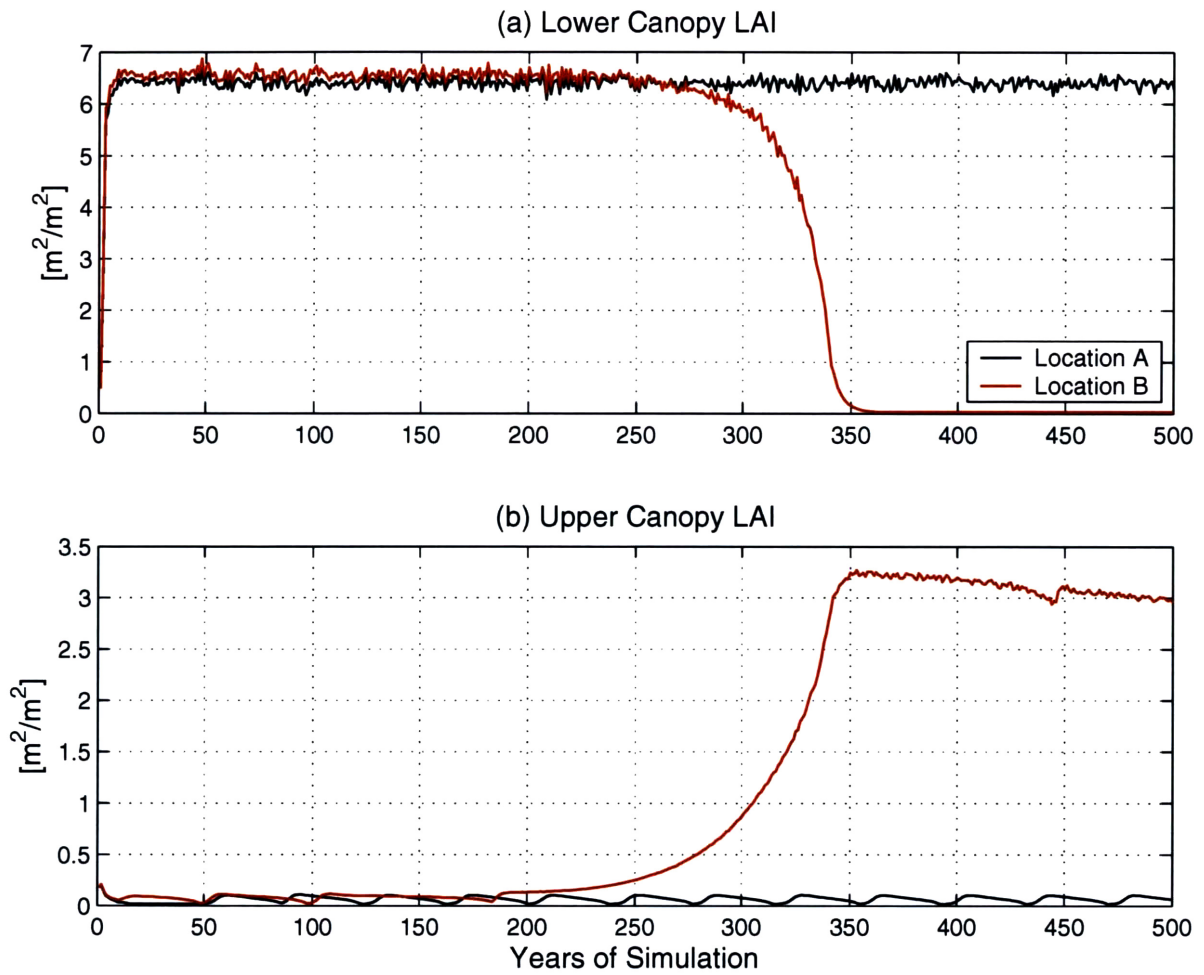


Figure 5-5: Change of (a) Lower Canopy LAI and (b) Upper Canopy LAI in response to the Different Groundwater Table Cycle at 11 °N

With both NCEP/NCAR and HAPEX-Sahel, the grasslands are simulated even with the shallowest water table of the results from SHE simulations, as presented in Figure 5-6 and 5-7. It suggests that the all grid cells of SHE in 13°N allow only grasses. No trees are allowed in the model even with the shallow water table.

In addition, the annual cycle of water table of NCEP/NCAR is more stable than that of HAPEX-Sahel. It is attributed to the characteristics of storm events, which are less intense and more frequent in NCEP/NCAR, as seen in Figure 3-3.

5.5 Discussion and Conclusion

The hypothesis is tested with the modified IBIS, including water table as a boundary variable that is taken from the simulated results of SHE. The asynchronous coupling of biospheric model and distributed hydrologic model is performed to validate the hypothesis, which is the variability of topography results in the spatial variation of soil moisture that can lead to the coexistence of trees and grasses in a region.

At 11°N, area of about 8% is covered by deciduous trees, and others by grasses. Savannas are defined as grasslands with the scattered trees covering less than 20% of the land surface (Wang, 2000). Hence, the experimental simulation results in the savanna ecosystems at 11°N, where savannas are observed in nature. For the region at 9°N, the model cannot simulate savannas. As addressed earlier, it is due to the limitation of the experimental design. Putting the water table in the land surface model acts as adding water on the model since the base simulation is done under the free gravitational condition. In the simulations with adjusting the rainfall input, it

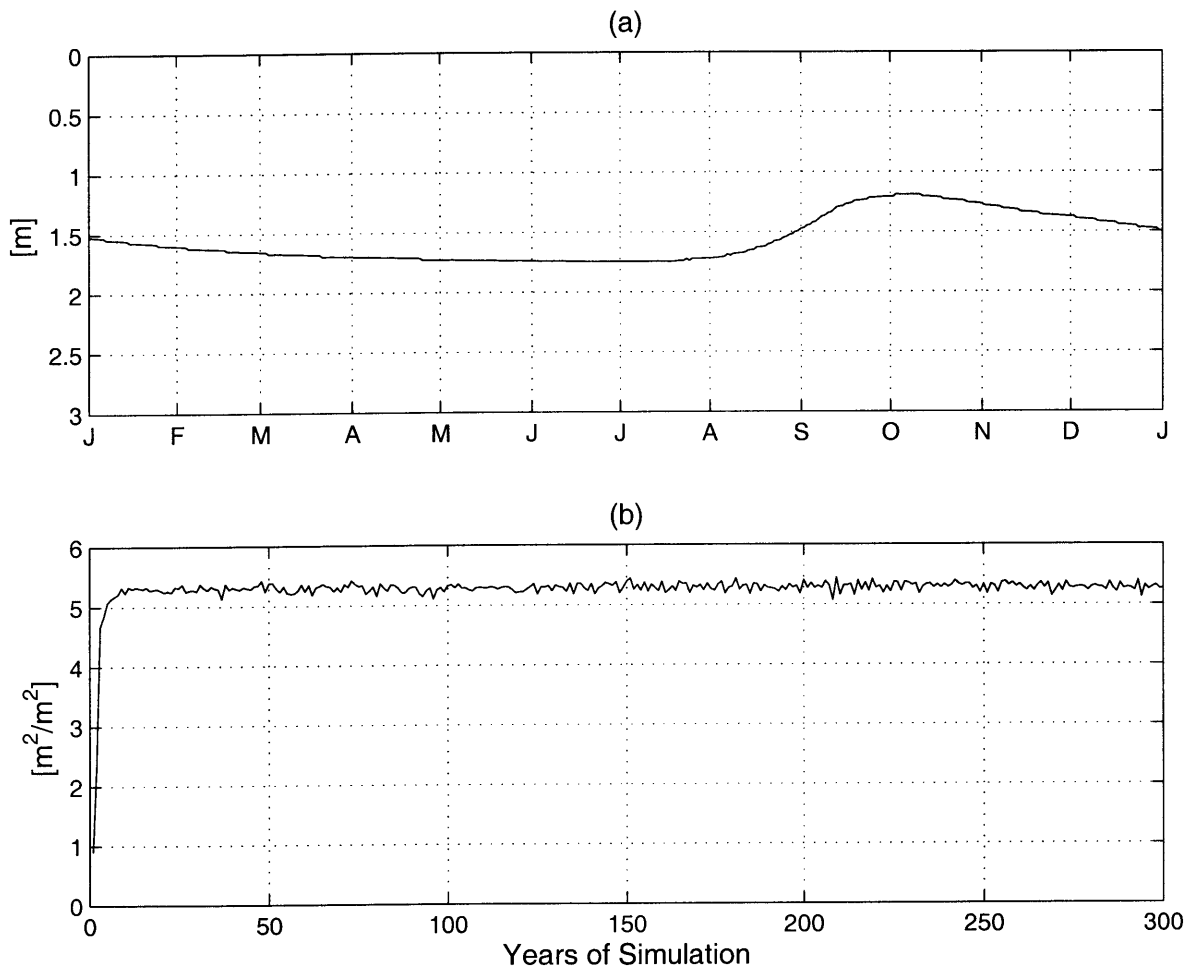


Figure 5-6: Change of (a) Shallowest Water table of SHE simulation, and (b) Lower Canopy LAI of IBIS with NCEP/NCAR at 13 °N

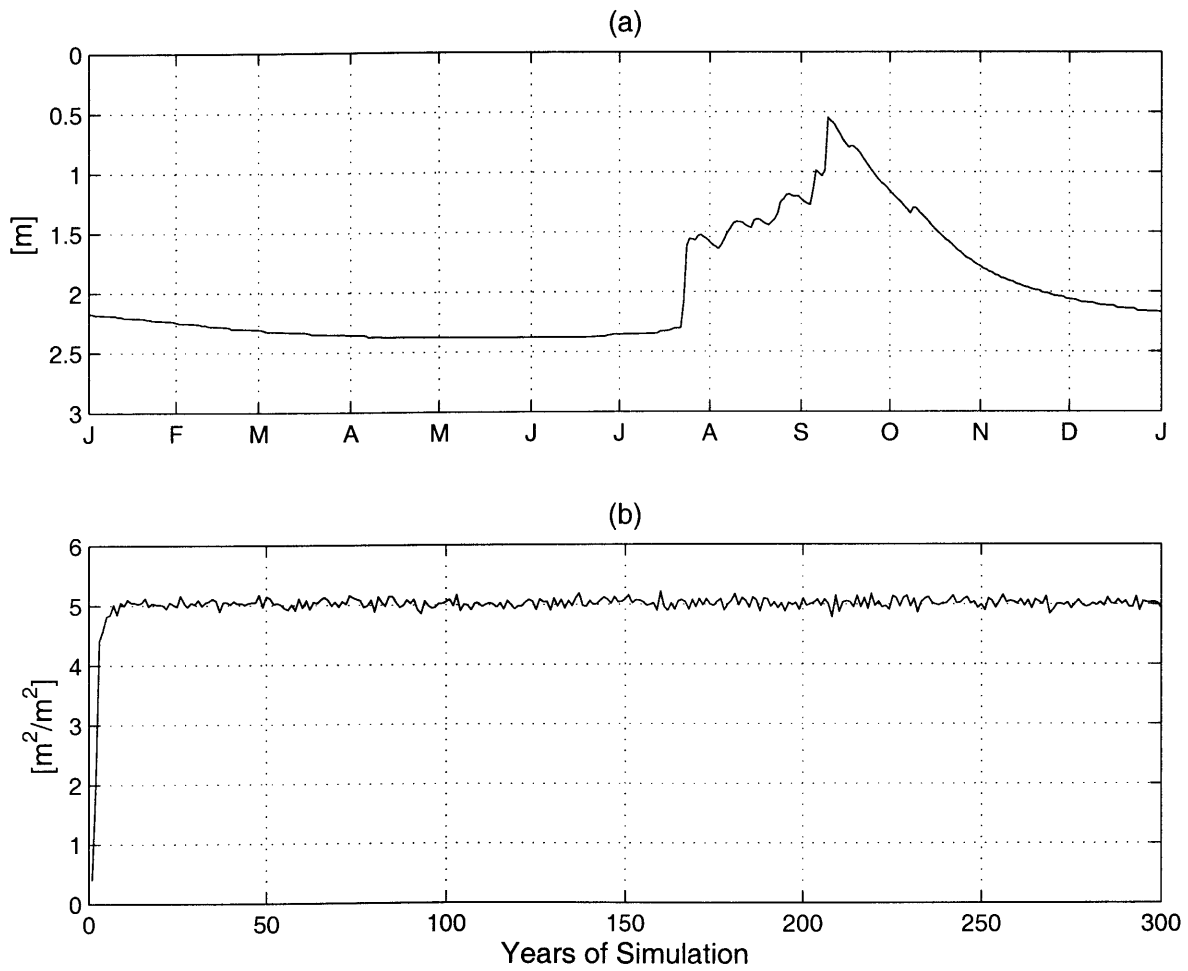


Figure 5-7: Change of (a) Shallowest Water table of SHE simulation, and (b) Lower Canopy LAI of IBIS with HAPEX-Sahel at 13 °N

is noted that the area in 9°N has grasslands as the amount of rainfall is decreased. Consequently, the design of simulation in this chapter cannot capture savannas at 9°N. At 13°N, grasslands are predicted regardless of water table depth, and it is consistent with the observation.

IBIS simulates grasslands both at 11°N and 13°N, assuming the soil bottom as a free drainage condition. Then by incorporating SHE and IBIS asynchronously, the model can simulate deciduous trees only in natural savannas of 11°N under the shallow water table depth (less than 2.6 *m*). At 13°N, trees are not supported even with the mean water table depth of around 1.6 *m* (in NCEP/NCAR). While adjusting the groundwater table depth, the model results in the different types of vegetation only in savannas. Thus the topographically induced variability of soil moisture can lead to the coexistence of trees and grasses under the savanna climate. The water availability plays a significant role on shaping savannas, and that can result from the variation of topography (exactly depth to water table). Even though soil moisture is important to dictate the vegetation type, this only can play a role under its climate of savannas. The shallowest mean water table depth (1.6 *m*) of 13 °N is enough to support trees at 11°N but not at 13°N. Hence the severe climate of natural grasslands may constrain the growth of trees in that region as noted in Chapter 3, as well.

The groundwater table depth of SHE is simulated under the assumption of bare soil. The existence of vegetation on land surface can adjust the annual cycle of water table depth. But our objective is to understand the role of water table on dictating the vegetation type, not the interaction between vegetation and water table.

Chapter 6

Conclusions

This thesis has addressed the question of how savannas emerge in general. Savannas can be shaped by many factors: fires and interannual variability of rainfall (which is falling in the disequilibrium view), and vertical/horizontal competition for water between trees and grasses (which is argued by the equilibrium view). In this study, it is hypothesized that a mixture of trees and grasses can exist due to the variability of soil moisture resulting from the variability of topography. This is validated with the biospheric model only, and by the asynchronous coupling of the biospheric model and distributed hydrologic model.

The experiment using the biospheric model is designed to estimate the amount of rainfall required for trees and grasses in a certain atmospheric condition. The difference of 30% in 9°N and 100% in 11°N is needed to simulate trees and grasses. Adjusting the rainfall amount can simulate the different types of vegetation only under savanna climate. It suggests that the availability of water is a important factor for trees and grasses to coexist at a certain climate window characteristic of savanna

	9°N	11°N	13°N
Observations	Savannas	Savannas	Grasslands
IBIS	Forests	Grasslands	Grasslands
Rainfall Variation with IBIS	Savannas	Savannas	Grasslands
Asynchronous Coupling of IBIS and SHE	N/A	Savannas	Grasslands

Table 6.1: Summarized Results

climate.

To understand the role of topography, distributed hydrologic modeling has been performed and we conclude that the variation of depth to water table, resulting from the variability of elevation, influences the variability of soil moisture to a high degree. Therefore IBIS is modified to include the groundwater table as a boundary variable, and the simulations are performed with the various water table taken from the results of SHE. The results of asynchronous coupling of SHE and IBIS through the groundwater table suggests that the different mean depth to water table can support the coexistence of trees and grasses only under the climate of savannas at 11°N. Table 6.1 presents the results of experiments addressed in this thesis, showing the designed experiments simulate savannas consistent with observations, and validating the proposed hypothesis. The findings in this study are summarized in the following:

- Different conditions of soil moisture can support different types of vegetation, trees and grasses, only for a certain savanna atmospheric climate.
- Grasses around 13°N cannot develop into trees even with increased soil moisture.

In other words, its severe atmospheric conditions limit the growth of trees.

- The variability of topography results in the variation of soil moisture through the variation in depth of groundwater table.
- The variability of water table resulting in the spatial variation of soil moisture can be a shaping factor of savannas.

The hypothesis predicts that a model can simulate a mixture of trees and grasses in response to the variation of topography in natural savannas. However, there are no currently available models that can fully describe the complex hydrologic processes including the dynamics of vegetation. Most distributed hydrologic models do not parameterize vegetation as a dynamic component. For instance, the SHE has a vegetation component, but leaf area index (LAI) and root density function (RDF) should be prescribed. Although the interaction between soil moisture and vegetation is evident, it is usually ignored, and some of models only concentrate on the one-way processes from vegetation to soil moisture. On the other hand, the dynamic vegetation models do not include the detailed hydrologic processes as well. The IBIS, used in this study, is one-column model and is developed for global scale studies within climate models. However, SHE includes the vegetation component using LAI and RDF (which are preliminary requirements for coupling with the ecosystem model (Arora, 2002)), and does not use the empirical function to estimate the evapotranspiration like most distributed models. Hence it can be coupled with the soil-plant-atmosphere model DAISY to calculate changes in crop yield, or leaching nitrate and pesticide. Even the linked model of SHE and DAISY cannot simulate the vegetation as a dynamic component, the coupling of SHE and vegetation dynamics will be possible with

the proper parameterization of vegetation and allocation scheme, used in IBIS. The necessity of the coupled model increases to better understand the natural processes , and Arora (2002) illustrates the manner how the coupling of vegetation models and hydrologic models can be performed. The development of the fully coupled model will give a chance to understand the interplay between soil moisture and vegetation dynamics as well as to study the hypothesis on emergence of savannas.

References

- Abbott, M. B., Bathurst, J. C., O'Connel, P. E., & Rasmussen, J. 1986a. An Introduction to the European Hydrological System - System Hydrologique Europeen "SHE", 1: History and Philosophy of a Physically-Based Distributed Modelling System. *Journal of Hydrology*, **87**, 45-59.
- Abbott, M. B., Bathurst, J. C., O'Connel, P. E., & Rasmussen, J. 1986b. An Introduction to the European Hydrological System - System Hydrologique Europeen "SHE", 2: Structure of a Physically-Based Distributed Modelling System. *Journal of Hydrology*, **87**, 61-77.
- Anderson, J.R., Hardy, E.E., Roach, J.T., & Witmer, R.E. 1976. *A Land Use and Land Cover Classification System for Use with Remote Sensor Data*. U.S. Geological Survey Professional Paper 964. Reston, VA: U.S. Geological Survey.
- Arora, V. K. 2002. Modelling Vegetation as a Dynamic Component in Soil-Vegetation-Atmosphere-Transfer Schemes and Hydrological Models. *Reviews of Geophysics*, **40**(2), 1006.

- Baven, K. J., & Kirby, M. J. 1979. A Physically Based, Variable Contributing Area Model in Basin Hydrology. *Hydrological Sciences Bulletin*, **24**, 43–69.
- Boone, A., & Wetzel, P. J. 1996. Issues Related to Low Resolution Modeling of Soil Moisture: Experience with the PLACE model. *Global and Planetary Change*, **13**, 161–181.
- Bourliere, F., & Hadley, M. 1983. *Present-day Savannas: Overview in Ecosystem of the World - Tropical Savannas*. New York: Elsevier Science Publishing Company.
- Brooks, R. H., & Corey, A.T. 1966. Properties of Porous Media Affecting Fluid Flow. *Journal of Irrigation and Drainage Engineering*, **92**(IR2).
- Casper, B. B., & Jackson, R. B. 1997. Plant Competition Underground. *Annual Review of Ecology and Systematics*, **28**, 545–570.
- Eagleson, P. S., & Segarra, R. I. 1985. Water-Limited Equilibrium os Savanna Vegetation Systems. *Water Resources Research*, **21**(10), 1483–1493.
- Foley, J. A., Prentice, C., Ramankutty, N., Levis, S., Pollard, D., Stich, S., & Haxeltine, A. 1996. An Integrated Biosphere Modle of Land Surface Processes, Terrestrial Carbon Balance, and Vegetation Dynamics. *Global Biogeochemical Cycles*, **10**(4), 603–628.
- Freeze, R. A., & Cherry, J. A. 1979. *Groundwater*. New Jersey: Prentice-Hall.
- Goutorbe, J. P. 1997. *HAPEX-Sahel*. Amsterdam, The Netheralnds: Elsevier Science B. V.

- Kiang, J. E., & Eltahir, E. A. B. 1999. Role of Ecosystem Dynamics in Biosphere-Atmosphere Interaction over the Coastal Region of West Africa. *Journal of Geophysical Research*, **104**(D24), 31,173–31,189.
- Pollard, D., & Thompson, S. L. 1995. Use of a Land-Surface-Transfer Scheme (LSX) in a Global Climate Model: the Response to Doubling Stomatal Resistance. *Global and Planetary Change*, **10**, 129–161.
- Rawls, W. J., Brakensiek, D. L., & Shirmohammadi, A. 1992. *Infiltration and Soil Water Movement: Handbook of Hydrology*. New York: McGraw-Hill.
- Rodriguez-Iturbe, I., & D'Odorico, P. 1999. Tree-Grass Coexistence in Savannas: The Role of Spatial Dynamics and Climate Fluctuations. *Geophysical Research Letters*, **26**(2), 247–250.
- Scholes, R. J., & Walker, B. H. 1993. *An African Savanna, Synthesis of the Nylsvley Study*. Cambridge, U. K.: Cambridge University Press.
- Skarpe, C. 1992. Dynamics of Savanna Ecosystems. *Journal of Vegetation Science*, **3**, 293–300.
- Thompson, S. L., & Pollard, D. 1995a. A Global Climate Model (GENESIS) with a Land-Surface Transfer Scheme (LSX). Part 1: Present Climate Simulation. *Journal of Climate*, **8**, 732–761.
- Thompson, S. L., & Pollard, D. 1995b. A Global Climate Model (GENESIS) with a Land-Surface Transfer Scheme (LSX). Part 2: CO₂ Sensitivity. *Journal of Climate*, **8**, 1104–1121.

- Walker, B. H., Holling, C.S., & Peterman, R. M. 1981. Stability of Semi-Arid Savanna Grazing Systems. *Journal of Ecology*, **69**(2), 473–498.
- Walter, H. 1971. *Ecology of Tropical and Subtropical Vegetation*. Edinburgh: Oliver and Boyd.
- Wang, G. 2000 (Feb.). *The Role of Vegetation Dynamics in the Climate of West Africa*. PhD Dissertation, Massachusetts Institute of Technology, Department of Civil and Environmental Engineering.
- Wang, G., & Eltahir, E. A. B. 2000a. Biosphere-Atmosphere Interactions over West Africa. 1: Development and Validation of a Coupled Dynamic Model. *Quarterly Journal of the Royal Meteorological Society*, **126**, 1239–1260.
- Wang, G., & Eltahir, E. A. B. 2000b. Biosphere-Atmosphere Interactions over West Africa. 2: Multiple Climate Equilibria. *Quarterly Journal of the Royal Meteorological Society*, **126**, 1261–1280.
- Yeh, P. J. 2003 (Feb.). *Representation of Water Table Dynamics In a Land Surface Scheme: Observations, Models, and Analyses*. PhD Dissertation, Massachusetts Institute of Technology, Department of Civil and Environmental Engineering.